



저작자표시-비영리-변경금지 2.0 대한민국

이용자는 아래의 조건을 따르는 경우에 한하여 자유롭게

- 이 저작물을 복제, 배포, 전송, 전시, 공연 및 방송할 수 있습니다.

다음과 같은 조건을 따라야 합니다:



저작자표시. 귀하는 원저작자를 표시하여야 합니다.



비영리. 귀하는 이 저작물을 영리 목적으로 이용할 수 없습니다.



변경금지. 귀하는 이 저작물을 개작, 변형 또는 가공할 수 없습니다.

- 귀하는, 이 저작물의 재이용이나 배포의 경우, 이 저작물에 적용된 이용허락조건을 명확하게 나타내어야 합니다.
- 저작권자로부터 별도의 허가를 받으면 이러한 조건들은 적용되지 않습니다.

저작권법에 따른 이용자의 권리는 위의 내용에 의하여 영향을 받지 않습니다.

이것은 [이용허락규약\(Legal Code\)](#)을 이해하기 쉽게 요약한 것입니다.

[Disclaimer](#)

Ph.D. DISSERTATION

A Biosensor platform based on the Carbon
Nanotube Network for detecting antibody
antigen reaction

(항원 항체 반응을 탐지하기 위한 탄소나노튜브 바이
오 센서 플랫폼)

By

Jaheung Lim

February 2018

SCHOOL OF ELECTRICAL ENGINEERING AND COMPUTER SCIENCE
COLLEGE OF ENGINEERING
SEOUL NATIONAL UNIVERSITY

A Biosensor platform based on the Carbon Nanotube
Network for detecting antibody antigen

(항원 항체 반응을 탐지하기 위한 탄소나노튜브
바이오 센서 플랫폼)

指導教授 朴 榮 俊

이 論文을 工學博士 學位論文으로 提出함

2018 年 2 月

서울대학교 大學院

電氣-컴퓨터 工學部

林 載 興

林 載 興의 工學博士 學位論文을 認准함

2018 年 2 月

委員長	<u>이 종 호</u>	(印)
副委員長	<u>박 영 준</u>	(印)
委員	<u>정 준 호</u>	(印)
委員	<u>김 성 재</u>	(印)
委員	<u>신 동 식</u>	(印)

**A Biosensor platform based on the Carbon Nanotube
Network for detecting antibody antigen reaction**

by

Jaeheung Lim

Submitted to the School of Electrical Engineering and
Computer Science

in partial fulfillment of the requirements for the degree of
Doctor of Philosophy in Electrical Engineering

at

SEOUL NATIONAL UNIVERSITY

February 2018

© Seoul National University 2018

Committee in Charge:

Jong Ho Lee, Chairman

Young June Park, Vice-Chairman

Junho Chung

Sung Jae Kim

Dong-Sik Shin

Abstract

A Biosensor platform based on the Carbon Nanotube Network for detecting antibody antigen reaction

JAEHEUNG LIM

SCHOOL OF ELECTRICAL ENGINEERING AND

COMPUTER SCIENCE

COLLEGE OF ENGINEERING

SEOUL NATIONAL UNIVERSITY

In this dissertation, a biosensor platform based on the carbon nanotube network (CNN) to detect the biomolecules such as DNA or proteins (target biomarker) and to quantify the concentration of them is presented.

Three salient features of the platform can be summarized as;

First, the sensor device with the concentric electrode structure is fabricated by using the standard semiconductor process. The carbon nanotube (CNT) channel between the concentric electrodes is formed by the dip-coating method. And the enhancement of current stability and resistance uniformity of the

sensor are achieved by the thermal evaporation of the gold nanoparticle (AuNP) on the carbon nanotube channel.

Second, for application of the AuNP decorated CNT device as the protein biosensor, the antibody is immobilized on the AuNP by the surface treatment with the developed chemical protocols.

Third, to enhance the change of the current response (sensitivity) on the CNT channel due to the antibody-antigen reaction, the electrical and the chemical methods such as the transient measurement, the ACEF method, the length of linker and the deactivation of NHS ester are applied and introduced.

Through this research, the possibility of the protein biosensor platform based on CNT is pursued and shown. The sensor platform based on the electrical sensing is expected to be used in detecting various kinds of proteins with the sufficient sensitivity and reliability in real time.

Keywords: Carbon nanotube, Gold nanoparticle, Protein sensor, Immobilization of antibody, hepatoma, liver cancer.

Student Number: 2008-20957

Contents

Abstract	i
Contents	iii
List of Tables	v
List of Figures	v
Chapter 1	1
Introduction	1
1.1 Motivation	1
1.2 Sensor platform.....	5
1.3 Outline of the Dissertation.....	7
Chapter 2	8
Sensor device fabrication	8
2.1 Fabrication of the electrodes pattern	8
2.2 Dip coating for the channel formation.....	13
2.3 Decoration of the channel with the metal nanoparticles.....	18
2.4 Conclusion	24
Chapter 3	25
Development of the sensor platform for the Protein sensor	25
3.1 Introduction	25
3.2 The electrical measurement system.....	32
3.3 Preparation process for the antibody immobilization.....	36
3.3.1 Surface blocking.....	36
3.3.2 Surface functionalization.....	42
3.3.3 Activation of the NHS-ester	47
3.3.4 Immobilization of the antibody	51
3.4 Experiment results for the antibody-antigen reaction.....	53

3.5 Conclusion of chapter 3	57
Chapter 4.....	59
Strategy for enhancement of sensor performance	59
4.1 Transient measurement.....	61
4.2 Enhancing the specific binding event: ACEF (AC Electrothermal Flow)	66
4.3 Introduction of linker.....	69
4.4 NHS-ester deactivation.....	73
4.5 Conclusion of chapter 4.....	76
Chapter 5.....	80
Conclusion.....	80
5.1 Summary.....	80
5.2 Future work.....	82
References	84

List of Tables

Table 2-1 Process flow table of fabrication of the electrode pattern	10
Table 3-1 The process flow for the surface treatment of the CNN channel to immobilize the antibody	29

List of Figures

Figure 1-1 Conceptual illustration of device structure; The gold nanoparticle decorated carbon nanotube is considered as a versatile functional material due to its biocompatibility and well-known binding method to immobilize biomolecules and chemical molecules.....	4
Figure 1-2 (a) Conceptual illustration of structure of sensor array and sensor cell (b) Schematic diagram of device, concentric structure gives self-gating effect in the solution.....	6
Figure 2-1 Vertical structure of each process flow	11
Figure 2-2 (a) Schematic representation of the device structure. The part of array type sensor structure consists of island electrodes and enclosing electrode. (b) The photograph of the process completed wafer.....	12
Figure 2-3 (a) The photograph of holder for multiple device fabrication. It	

shows that the dip coating method is suitable process for the mass production. (b) The photograph of the dip coating machine	16
Figure 2-4 (a) Conceptual representation of the dip coating method with the CNT network (b) the resistance of the channel versus the ambient humidity during the dip coating condition.....	17
Figure 2-5 (a) Chamber inner structure consists of the metal source on the tungsten boat, substrate holder and shutters. (b) Tungsten boat contains the metal sources and voltage source raises temperature.....	20
Figure 2-6 A SEM view of the gold nanoparticles on the CNN surface.....	21
Figure 2-7 (a) Statistical distribution of the channel resistance: the bare CNN and the CNN decorated by the gold nanoparticle. The resistance of the CNN decorated by gold nanoparticle is stable over time. (b) Band diagram of the CNN and the gold.	22
Figure 2-8 (a) Statistical distribution of the channel resistance: the bare CNN and the CNN decorated with the aluminum nanoparticles. The change of the CNN decorated by aluminum nanoparticle over the storage time. (b) Band diagram of the CNN and the aluminum material	23
Figure 3-1 (a) A schematic illustration of the device structure for sensing the protein: The AuNP decorated CNN is integrated on the concentric electrodes and the antibody is immobilized on the AuNP. (b) The schematic illustration of the immobilized antibody after surface treatment of CNN channel	28
Figure 3-2 Schematic procedure of the surface treatment to immobilize antibody (a) bare device (b) the surface blocking: TWEEN20 (c) surface functionalization: MPA (d) activation of NHS ester (e) immobilization of antibody	30
Figure 3-3 Real-time measurement of the electrical current change during the	

<p>surface treatments including the surface blocking, surface functionalization, activation of NHS ester and immobilization of the antibody; all the values are normalized to the initial channel current in the PBS solution</p>	31
<p>Figure 3-4 (a) The component of the electrical measurement system: power supply, function generator, oscilloscope and the circuit board with the sensor device under test.</p>	34
<p>Figure 3-5 (a) Schematic circuit diagram of the CNN device in the buffer solution with the electrical measurement setup, (b) applied input bias voltage and (c) output voltage waveforms from the OPAMP versus time</p>	35
<p>Figure 3-6 (a) Structure of the TWEEN20 consists of the hydrophilic and hydrophobic region. (b) Schematic illustration of the TWEEN20 adsorbed to the CNT surface forming the blocking layer.....</p>	39
<p>Figure 3-7 Real-time measurement of current change during the surface blocking with 1% TWENN20 in PBS</p>	40
<p>Figure 3-8 (a) Schematic of a monolayer of TWEEN20 adsorbed on a nanotube, repelling nonspecific binding of proteins in solution. (b) Real-time measurement of sensor current during adsorption of the BSA; the bare device (black line), the device with the TWEEN20 (red line).....</p>	41
<p>Figure 3-9 (a) Structure of MPA (b) Schematic illustration of device surface modified with MPA</p>	44
<p>Figure 3-10 (a) Real time measurement of current change during MPA adsorption and washing process (b) Energy band diagram of the device; The current decreases after binding the MPA on the surface since the thiol-molecules reduce the work function of gold.</p>	45
<p>Figure 3-11 (a) Real time measurement of current change during the MPA</p>	

adsorption and washing process. Schematic illustration of the device structure with MPA on (b) the CNN device without the AuNP, (c) the AuNP decorated CNN device	46
Figure 3-12 (a) Schematic illustration of the MPA being converted to NHS ester by the reaction of EDC (b) Real time measurement of the current change during the EDC/NHS reaction.....	49
Figure 3-13 pH dependence of the channel current for various device structures; the CNN device (black), the AuNP decorated CNN device (red) and the MPA on the AuNP (blue).....	50
Figure 3-14 (a) The amine group of the antibody can be linked to the NHS ester on the gold nanoparticle. (b) Real time measurement of current change during the antibody immobilization on the NHS ester site at the MPA linker molecule.....	52
Figure 3-15 Real time measurement of current change during the specific binding (AFP) and nonspecific binding (BSA) events.	55
Figure 3-16 The rate of current changes for various concentrations of specific and nonspecific molecules. The data for the PBS and serum conditions are also shown.....	56
Figure 4-1 Schematic illustration of transient measurement method; There exists a space charge layer at the interface between the solution and the protein, which screens the electrostatic field induced from the charged molecule over the Debye length. After the step-pulse bias, the Debye length is extended instantaneously, the screening counter-ions around the target molecule are swept away during the transient state.....	63
Figure 4-2 (a) schematic diagram of current component of the device in the solution (b) the output voltage when the step pulse is applied; (c) the channel current; the CNT current can be calculated by subtracting the	

discharging current from the charging current.....	64
Figure 4-3 Comparison of the current change between the transient state and the steady state; the difference between steady state current and the transient state current is negligible for the cut-off concentration of AFP (1ug/ml).....	65
Figure 4-4 The rate of current changes when the ACEF method is applied for various conditions; there is no difference in the current change between specific binding and nonspecific binding. High temperature caused by the ACEF may lead to degradation of the binding efficiency due to deformation of the antibody proteins.	68
Figure 4-5 Schematic illustration of the effects of the linker materials; the MUA linker was substituted for the MPA linker to immobilize the antibody on the channel surface.....	71
Figure 4-6 Real time measurement of the current change during the reaction between the antibody and the 10 ug/ml of antigen AFP (a) MPA as a linker (b) MUA as a linker.....	72
Figure 4-7 Schematic illustration of the deactivation procedure; The remaining NHS esters after immobilization of antibody are deactivated with other proteins which have amine group.....	74
Figure 4-8 Real time measurement of the changes of current under deactivation of NHS ester by BSA; 1) The current change by nonspecific protein, such as BSA, decreases after deactivation. 2) It also diminishes the current change by AFP which is the target molecule.....	75
Figure 4-9 Schematic illustration of the DNA, aptamer and antibody immobilized on the AuNP decorated CNN device; 1) DNA or aptamer has an advantage to detect since its size is smaller than that of antibodies. 2) The binding region of probe is near the CNT surface that can be more	

affected by target molecule. 3) DNA and aptamer do not have
degradation in high temperature which is induced by joule heating in
ACEF.79

Chapter 1

Introduction

1.1 Motivation

The carbon nanotube (CNT) is a promising one-dimensional nanostructure for various nano-electronics applications. Compared with the conventional electronic devices, the device based on the CNT has high surface to volume ratio. This property is exploited to convert chemical and biological reactions on the device surface into changes of the electrical characteristics [1][2].

By using the semiconductor behavior of the CNT, the electrical biosensor platform with the CNT channel has been invented in our laboratory [3]. In the channel region of the device, the carbon nanotube network (CNN) is formed between the concentric electrodes. Additionally, the metal nanoparticles are decorated on the channel region as shown in figure 1-1. The process to form the CNN in the channel region of the device is the mask free (no need of an additional photolithography process) and the low temperature process. Since the device is fabricated with the standard CMOS fabrication process, it can be

easily integrated to the CMOS integrated circuit (IC). In the following, several important applications of the platform reported from our group will be summarized.

The integration of the palladium (Pd) decorated CNN sensor and CMOS IC to detect hydrogen gas in a single chip has been reported [4].

The threshold voltage of the device, which is estimated by measuring the changes of the channel conductance as the function of the gate voltage, is observed under the various concentration of the hydrogen ion (pH) in the solution [5].

Next, the sensor device has been developed as a biosensor application. The CNN channel region was decorated with the gold nanoparticle (AuNP) as the immobilization site of the probe DNA. The conductance of the gold nanoparticle decorated CNN device can be changed by the work function modulation which is caused by the probe DNA-target DNA hybridization [6]. It was found that the sensitivity of the device could be enhanced by applying the electrical pulse biasing during the hybridization process [7]. The device platform has been shown to operate properly as a DNA biosensor.

To detect the protein, which is Troponin I related to the cardiac infarction, the aptamer is selected as a probe molecule. Additionally, by adopting the electrothermal flow method, which is a kind of the electrokinetics, the

sensitivity of the device was enhanced [8].

In summary, the sensor platform in our laboratory, the device has been introduced as the gas sensor, the pH sensor, the DNA sensor and the protein-aptamer sensor except for the antibody as probe molecule. Therefore, it is the purpose of this dissertation to extend the device application to the protein sensor platform by applying the antibody as the probe molecule.

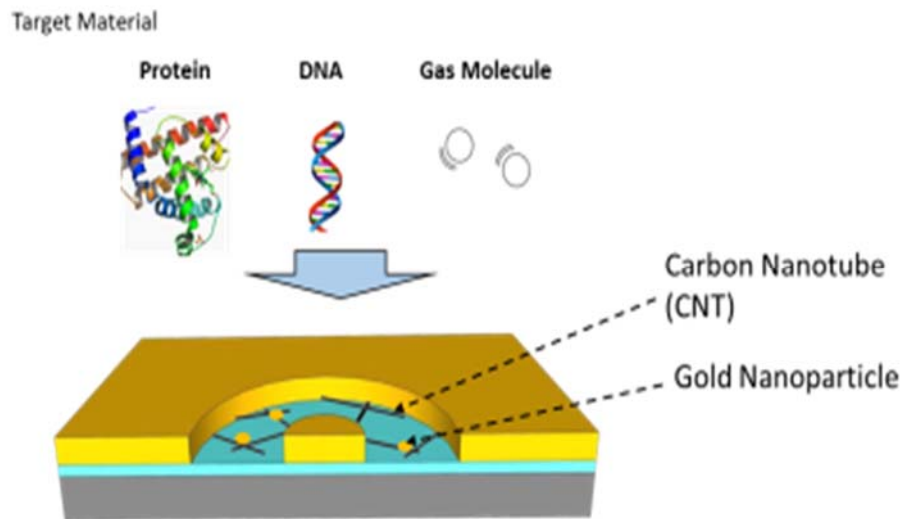


Figure 1-1 Conceptual illustration of device structure; The gold nanoparticle decorated carbon nanotube is considered as a versatile functional material due to its biocompatibility and well-known binding method to immobilize biomolecules and chemical molecules.

1.2 Sensor platform

In general, most conventional electrode structure used in the biosensor platform is parallel plates or an interdigitated-comb structure. The structure of the device in this work adopted the asymmetric and concentric structure where the small island electrode is surrounded by the large enclosing electrode.

Figure 1-2(a) shows the concept of the concentric electrode structure. The concentric electrode consists of the island electrode (inner circle) and the enclosing electrode (outer plane). The CNN is formed on the channel area between concentric electrodes by dip coating method. As shown in figure 1-2(b), due to the much larger area of enclosing electrode than that of island electrode, the electrostatic potential of the solution is determined by the potential applied to the enclosing electrode, which is originated from a capacitive coupling of the electric double layer, when the device is immersed in the solution. Therefore, the current of device is measured in the solution by using two electrodes without external electrode. The phenomenon has been reported under the name of the ‘self-gating effect’ [3].

The channel region is composed of the CNN and the metal nanoparticle. The electrical characteristic of the CNN can be changed by the metal species deposited on the CNN surface. When the device is used to the biosensor application, the AuNP is selected to provide the binding sites for the probe

molecules.

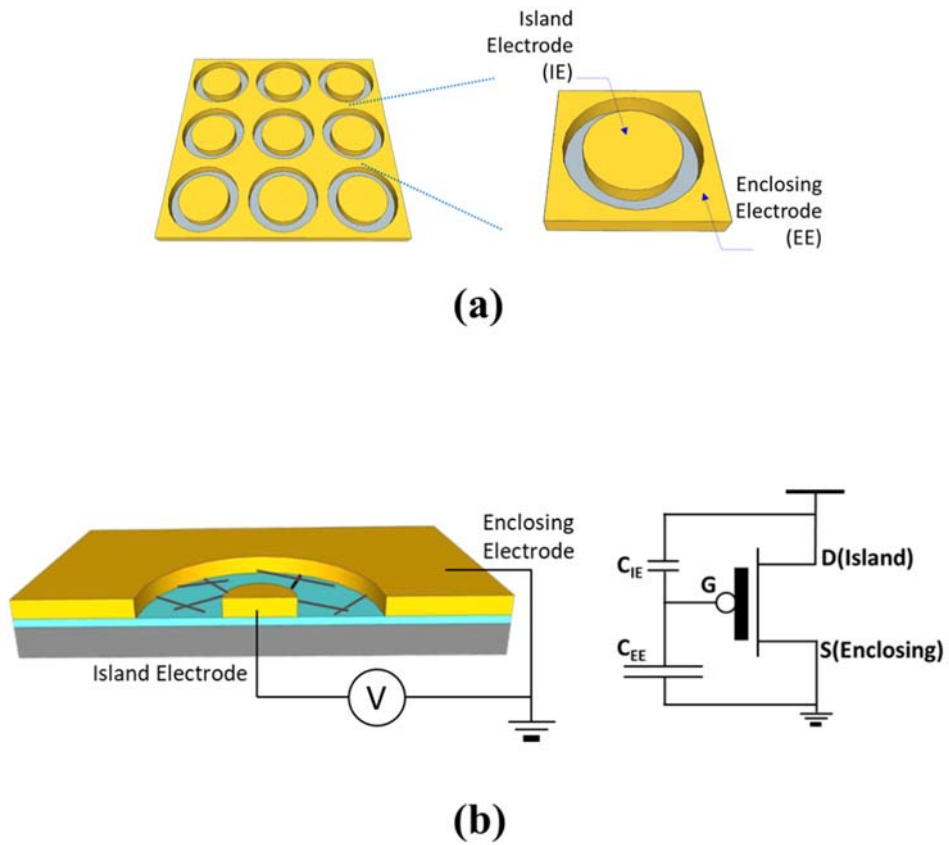


Figure 1-2 (a) Conceptual illustration of structure of sensor array and sensor cell (b) Schematic diagram of device, concentric structure gives self-gating effect in the solution

1.3 Outline of the Dissertation

The primary purpose of the dissertation is to develop the CNT based biosensor device and optimize the protocol of the surface treatment of the channel for enhancing the performance of the device platform. Additionally the physical and the electrical characteristics of the CNT are understood through the preparation of the protein sensor device.

In chapter 2, the basic fabrication process of the sensor device, the CNT channel formation by using the dip-coating method and deposition of the gold nanoparticle by thermal evaporation are described.

In chapter 3, the immobilization process of the antibody for detecting the target protein is introduced. The process consists of four procedures: 1) the surface blocking, 2) the functionalization of the surface with the linker molecule, 3) the activation of the functional group and 4) the immobilization of the antibody.

In chapter 4, the electrical and the chemical methods to enhancing the sensor performance are explained. The detail procedure and their experimental results are shown.

In chapter 5, the conclusion of the present work is given together with the summary for the future study.

Chapter 2

Sensor device fabrication

In this chapter, the fabrication process of the device platform will be described. This device has the unique feature of the concentric electrode structure; the island electrode and the common electrode enclosing the island electrode. The gap region between the two electrodes becomes the channel region of the CNT-FET. The channel region consists of the carbon nanotube network (CNN) as the electrical channel and gold nanoparticle. The CNN can be easily fabricated by dip coating method and gold nanoparticle is deposited by the thermal evaporation. In addition, the effects of various metal nanoparticle decoration on the CNN channel will be discussed.

2.1 Fabrication of the electrodes pattern

A conventional metal process in the semiconductor chip is used to form the concentric electrode structure. Table 2-1 and figure 2-1 summarize the total process flow in the device fabrication.

In the first step, the residual organic materials and metal impurities on the wafers were removed by the SPM (Sulfuric acid Peroxide Mixture) cleaning, SC-1 (Standard Cleaning-1) NH_4OH solution and SC-2 (Standard Cleaning-2) HCl solution. And it is the optional sequence that silicon wafer is cleaned by the HF (hydrofluoric acid) solution to obtain a surface free of native oxide.

Next the silicon oxide (SiO_2) was grown by the high temperature wet oxidation process (900°C for 10 hr, for the thickness of $1\ \mu\text{m}$) in order to make insulation layer on the silicon surface.

Photo process and metal evaporation process for electrode structure were conducted. The electrode was composed titanium (Ti) $500\ \text{Å}$ and gold (Au) $2000\ \text{Å}$, where titanium acts as an adhesion enhancement metal to help deposition of the gold on the oxide surface.

After deposition process of the electrode metals, the ultrasonication process was performed for 30 minutes to remove the negative photoresistor, and then the concentric electrode structure was revealed. The array of the concentric electrode structure with $10\ \mu\text{m}$ channel length and $50\ \mu\text{m}$ diameter of the island electrode was formed as shown in figure 2-2.

SEQ.	Process	Condition
10	SPM cleaning	
20	SC-1,2 cleaning	
30	CMOS furnace (Wet oxidation)	SiO ₂ 1μm
40	Spin coating	Negative PR
50	Aligner(MA6-III)	
60	WS-18A, Develop	
70	E-gun Evaporator	Ti: 500A, Au:2000A
80	Lift off	Acetone 30min.
90	Dicing Saw	

Table 2-1 Process flow table of fabrication of the electrode pattern

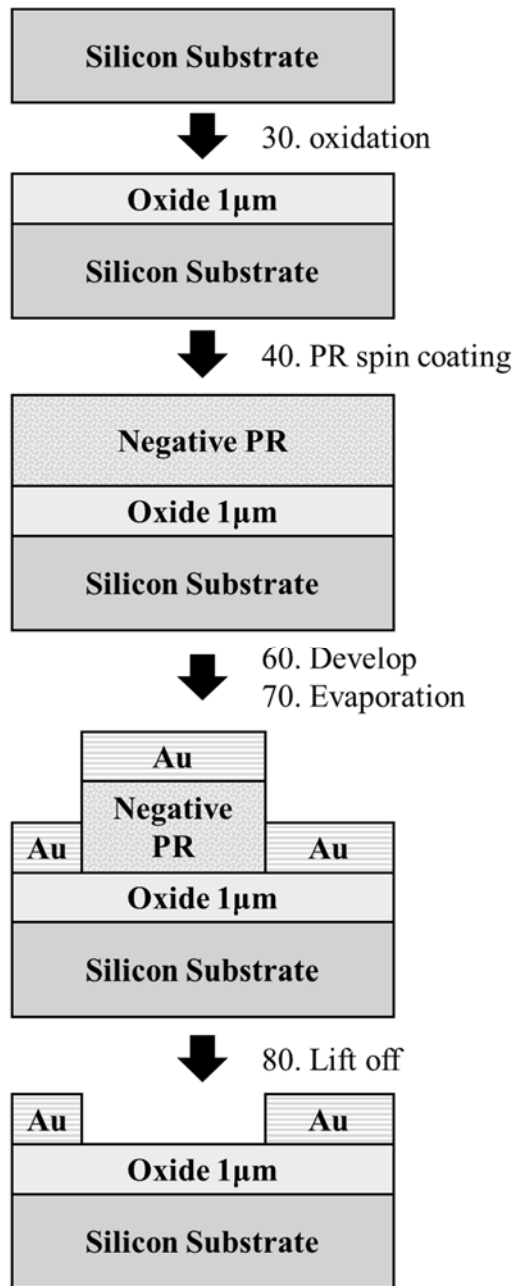


Figure 2-1 Vertical structure of each process flow

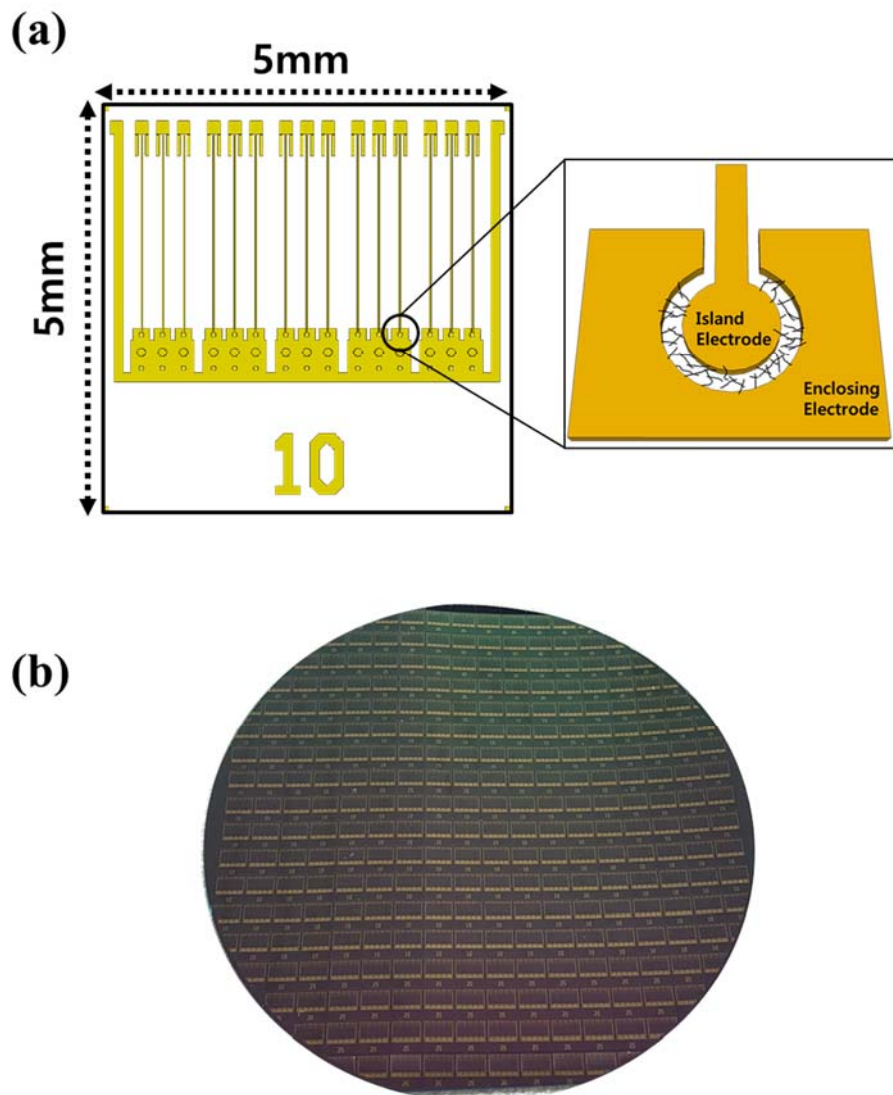


Figure 2-2 (a) Schematic representation of the device structure. The part of array type sensor structure consists of island electrodes and enclosing electrode. (b) The photograph of the process completed wafer.

2.2 Dip coating for the channel formation

There are several approaches for deposition of the carbon nanotube on the substrate. They are the spray coating [9], spin coating [10] and dip coating [11]. The spray coating and spin coating are a simple method but they are hard to obtain uniform network. The dip coating method makes up for the uniformity problem in other methods and it is a suitable process for mass production as shown in figure 2-3. Accordingly, the dip coating method is used for formation of the carbon nanotube channel between the island electrode and enclosing electrode. It is necessary to prepare the sufficient dispersed carbon nanotube solution to obtain the uniformly distributed CNT network film on the substrate. Because the pristine form of the CNT is a bundle due to the van der Waals interaction, the raw CNT needs to be pretreated with nitric acid oxidation to disperse in an organic solvent.

In this work, the unpurified CNT powder (ASP-100F produced by Iljin Nanotech, Korea) was ultrasonicated in the nitric acid at 50°C for 30 min to purify and separate tube from bundle. This treatment helps to produce the carboxyl acid group and hydroxyl group on the CNT surface and stabilize the CNT suspension in the solvent. The CNT in the nitric acid was neutralized three times with the deionized water (DIW) and then concentrated by on the membrane filter paper (Millipore, 0.2 μm pore size, 47 mm diameter) in the

vacuum filtration system. The concentrated CNT powder on the filter paper was dried in a vacuum condition at 80°C for 24 hr. This pretreated CNT was inserted in the 1,2-dichlorobenzene solution (ReagentPlus®, 99%, D56802, Sigma-Aldrich, Korea) with a concentration of 0.01 mg/ml, and ultrasonication process is performed to homogeneously disperse the carbon nanotube colloidal solution for 30 min [11]. The CNT colloidal solution with the 1,2-dichlorobenzene could be preserved for over 6 months without aggregation.

For the formation of the channel between the two electrodes, the CNN is deposited through the dip coating process, where the chip is immersed into and then drawn out of carbon nanotube dispersed the 1,2-dichlorobenzene solution at a constant withdraw velocity of 1.5 mm/min as shown in Fig 2-4(a). The mechanism of the channel formation is that the capillary force caused by evaporation of the solution makes the solution flow into the surface, and then the CNN is formed on the substrate. In this way, a self interconnecting between the island electrode and the enclosing electrode is achieved. Since the rate of evaporation is affected by the ambient humidity, the conductance of the channel, which is determined by the density of CNT, decreases as the ambient humidity increases. The relationships between the resistance and the ambient humidity are shown in figure 2-4(b). On the other hand, as shown in figure 2-4(b), it is interesting to notice that the resistance of the channel shows little

dependence on the ambient humidity when an oxygen plasma treatment was performed to the device for 5 minutes in 500 W of RF power. This is because the density of CNT increases due to the surface polarity of oxide layer changed by the oxygen plasma treatment [12]. This dip coating method leads to the ohmic contact between the CNN and the gold concentric electrode, whose work functions are 4.8 eV and 5.2 eV, respectively. More detailed explanation about the work function is presented in the next section 2.3.

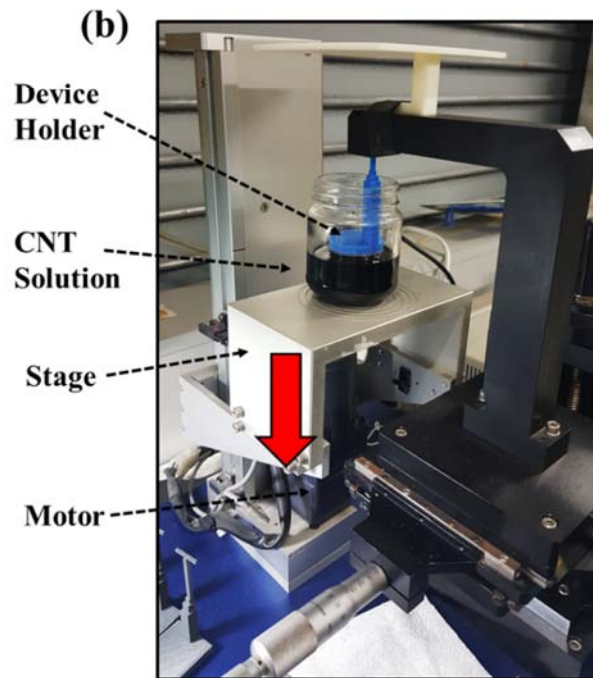
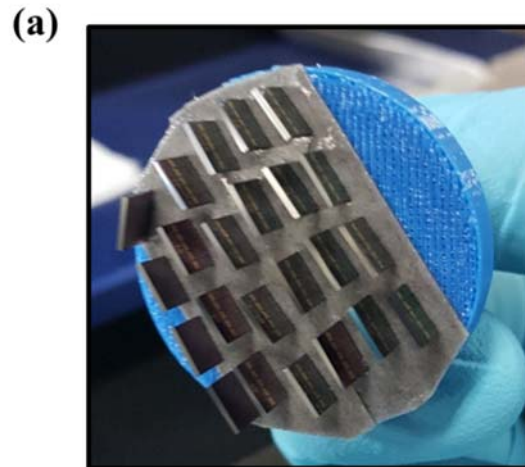


Figure 2-3 (a) The photograph of holder for multiple device fabrication. It shows that the dip coating method is suitable process for the mass production.

(b) The photograph of the dip coating machine

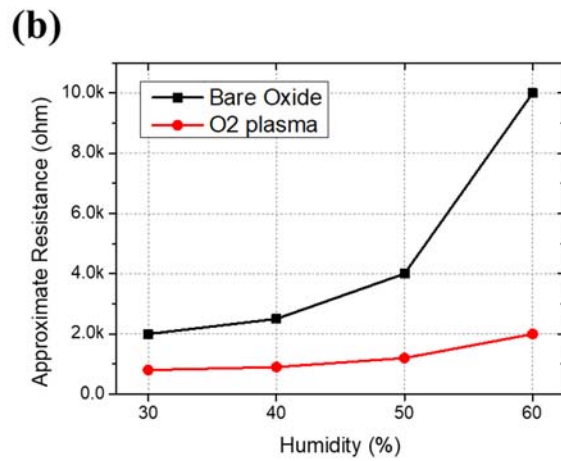
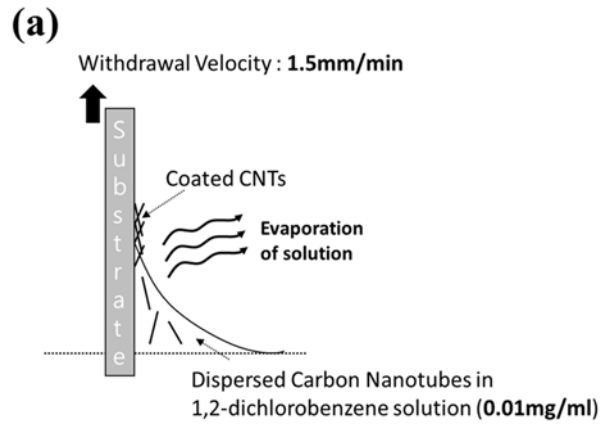


Figure 2-4 (a) Conceptual representation of the dip coating method with the CNT network (b) the resistance of the channel versus the ambient humidity during the dip coating condition

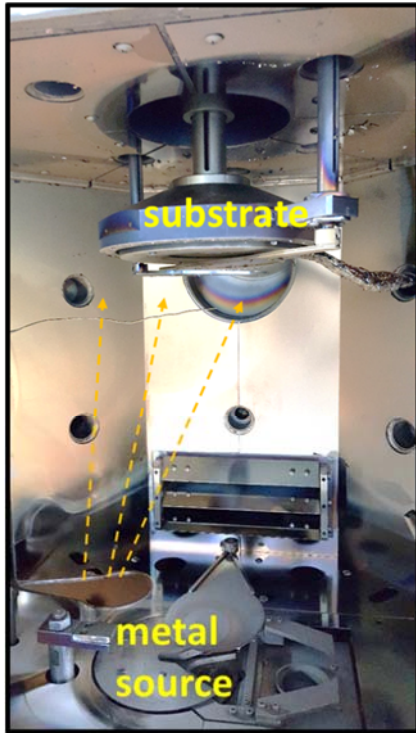
2.3 Decoration of the channel with the metal nanoparticles

Decoration of the metal nanoparticle on the CNN is performed by a thermal evaporation method which provides a simple way to deposit the uniformly distributed metal nanoparticle [13]. The detail processing conditions to decorate the nanoparticle are as follows. The pressure in the evaporation chamber is pumped down to 2.0×10^{-2} Torr by a rotary pump, and followed by pumping down to 9.0×10^{-6} Torr by a turbomolecular pump. After the pressure is stabilized, a voltage is applied across the tungsten boat filament containing the metal sources to raise temperature as shown in figure 2-5. The deposition rate and thickness are monitored using a quartz crystal microbalance (QCM) and the thickness measured by the QCM is obtained as the frequency changes with the deposition thickness on the quartz substrate [14]. In this work, the thickness of all the metal nanoparticle is adjusted to be 1nm at 1 Å/sec of deposition rate in 10 seconds. For example, figure 2-6 shows a SEM (Scanning Electron Microscope) image of the gold nanoparticle deposited on the CNN surface.

To understand the relationship between the conductance of the CNN and the work function of metal nanoparticle, the CNN channels are decorated with the gold (Au) and aluminum (Al) which have the work function of 5.2 eV and 4.1 eV, respectively.

In the case of the CNN decorated by the gold nanoparticle, since the work function of gold is higher than that of CNN (4.8 eV), the hole carriers at the CNN surface are accumulated, which causes the decrease of the channel resistance about 35% as shown in figure 2-7. The reliable channel resistance over 1 month is observed when the devices are kept in normal air condition.

On the other hand, in the case of the CNN decorated by the aluminum nanoparticle, since the work function of aluminum is smaller than that of CNN, the hole carriers at the CNN surface are depleted, which causes the increase of the channel resistance about 10 times as shown in figure 2-8. Additionally, the channel resistance decreases over time in the normal ambient condition because air exposed aluminum is naturally oxidized to aluminum oxide (Al_2O_3) which is higher than the work function of aluminum [15].



(a)



(b)

Figure 2-5 (a) Chamber inner structure consists of the metal source on the tungsten boat, substrate holder and shutters. (b) Tungsten boat contains the metal sources and voltage source raises temperature

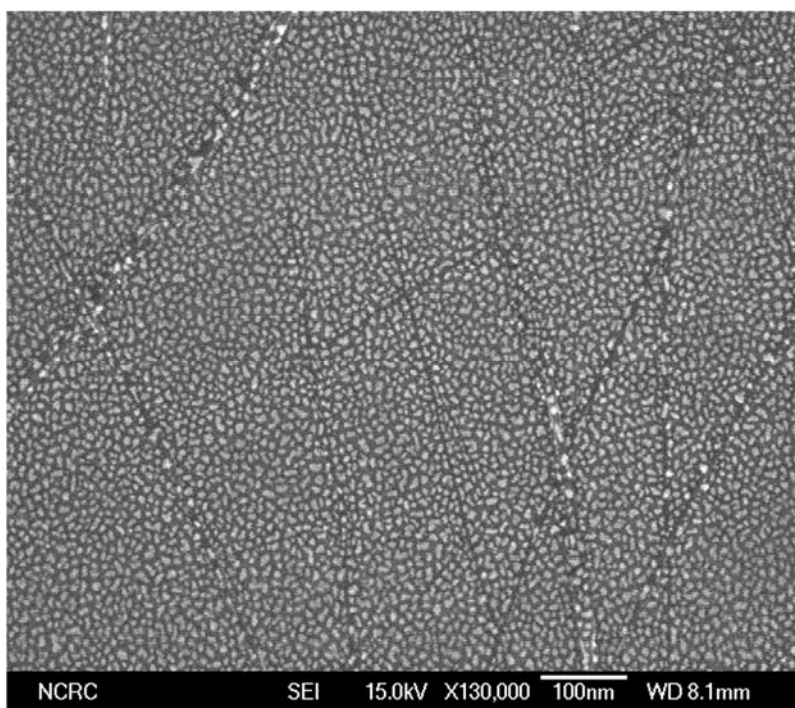
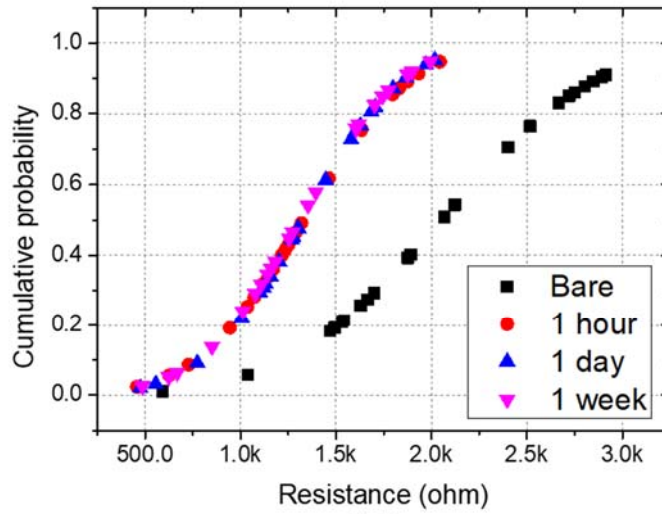
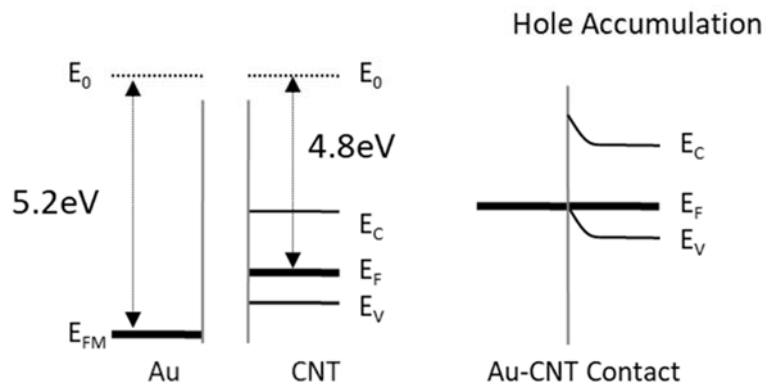


Figure 2-6 A SEM view of the gold nanoparticles on the CNN surface

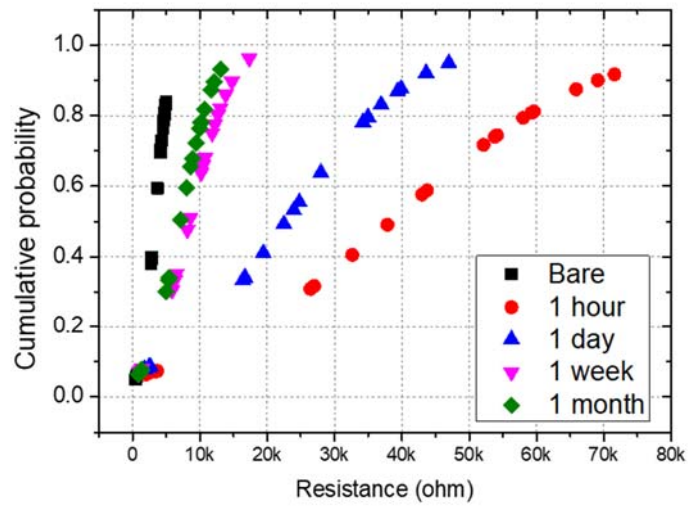


(a)

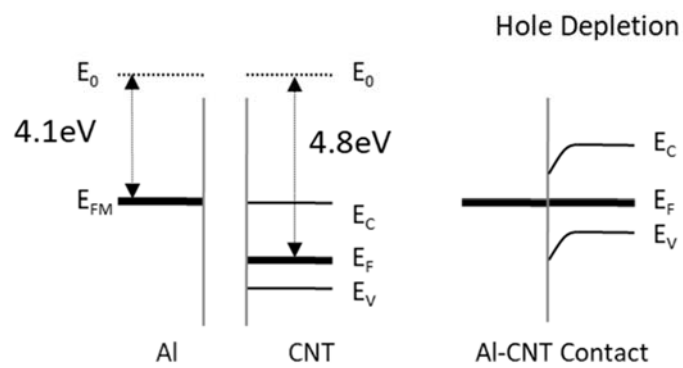


(b)

Figure 2-7 (a) Statistical distribution of the channel resistance: the bare CNN and the CNN decorated by the gold nanoparticle. The resistance of the CNN decorated by gold nanoparticle is stable over time. (b) Band diagram of the CNN and the gold.



(a)



(b)

Figure 2-8 (a) Statistical distribution of the channel resistance: the bare CNN and the CNN decorated with the aluminum nanoparticles. The change of the CNN decorated by aluminum nanoparticle over the storage time. (b) Band diagram of the CNN and the aluminum material

2.4 Conclusion

In this chapter, the fabrication of the electrode, the formation of the CNT channel using the dip coating method and the decoration of metal nanoparticle on the CNT surface have been introduced.

The dip coating method with the concentric electrode provides an array structure of the CNN and is suitable for a mass production without extra process such as photolithography and etching. And the method of decoration of the CNN channel with the metal nanoparticle by thermal evaporator can form the gold particles with nano size. It is shown that the change of the channel resistance is caused by the modulation of the surface potential of the CNN channel by the work function difference between the metal particles and the CNN channel. Especially, the gold nanoparticle decorated CNN shows highly uniformity and stability in the channel resistance.

With the presented procedures, the electrical channel has been prepared for the following implementation of the bio specific treatment in the next chapter for the biosensor detecting biochemical reaction.

Chapter 3

Development of the sensor platform for the Protein sensor

3.1 Introduction

In this chapter, the sensor platform for the detection of alpha fetoprotein (AFP), which is known as the biomarker related with the hepatoma (liver cancer) [16], were constructed and analyzed. For the application of the CNN decorated by the gold nanoparticle device (CGi) to the protein sensing, the antibody is adopted the probe molecule to bind with the target protein, as shown in figure 3-1. The binding reaction between antibody and target protein molecule leads to the change of channel current, which is the indicator to estimate the amount of the bound protein, related with the concentration of the target proteins in the solution.

The antibody can be immobilized on the AuNP through a linker formed by the surface treatment. Table 3-1 summarizes the flow of the surface treatment process including the surface blocking, surface functionalization, activation of

the NHS ester and immobilization of the antibody.

First, the TWEEN20 was applied to avoid the nonspecific binding with the noisy (the non-target proteins which may present in the solution) proteins, which may be adsorbed to the surface of the CNN and that of the AuNP, due to the hydrophobicity of the molecules [17]. The 3-mercaptopropionic acid (MPA), which contains the carboxyl functional group, is formed on the AuNP as a linker. And the mixture of EDC/NHS (EDC:1-(3-Dimethylaminopropyl)-3-ethylcarbodiimide/NHS:N-hydroxysulfosuccinimide) converts the carboxyl group of the MPA to the amine-reactive NHS esters. Thus, the amine group of the protein can be linked to the NHS ester of the MPA by the covalent bonding. The schematic procedure of the surface treatment for the immobilization of the antibody is shown in figure 3-2.

The change of the electrical current during the surface treatment in each step may give important information in terms of the electrical characteristics of the AuNP on the CNN during being interacted with the chemicals in the solution. The steady state current under the pulsed voltage of 0.3 V applied to the drain (the island electrode) measured during the surface treatment in all steps as shown in figure 3-3.

In the following sections, the electrical measurement system for measuring the modulation of the electrical current is described. More detailed explanation

about the surface treatments is presented step by step. The experimental results of the reaction after the immobilization of antibody under various conditions which leads to the change of current are shown. The overall electrical data after the binding events will provide the means of testing the feasibility of the platform.

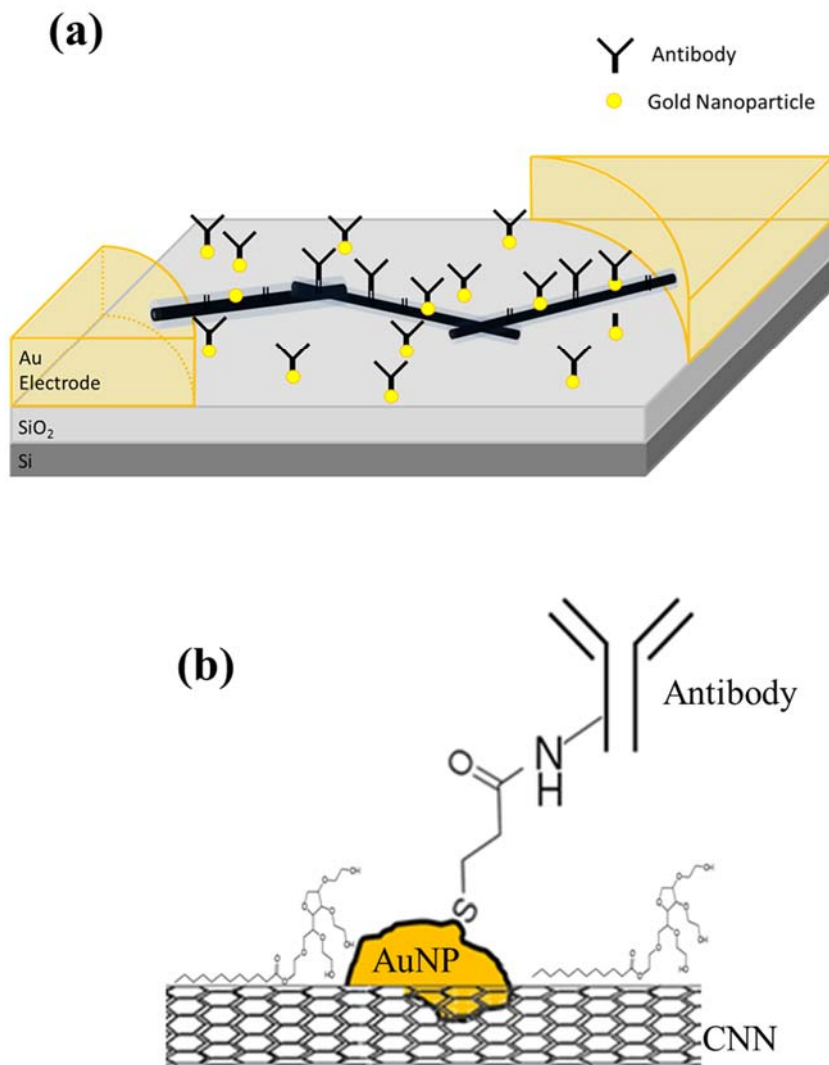


Figure 3-1 (a) A schematic illustration of the device structure for sensing the protein: The AuNP decorated CNN is integrated on the concentric electrodes and the antibody is immobilized on the AuNP. (b) The schematic illustration of the immobilized antibody after surface treatment of CNN channel

SEQ.	Process	Condition	Description
10	Bare device		The AuNP decorated carbon nanotube
20	Surface blocking	1% TWEEN20 in PBS	TWEEN20 layer to block the nonspecific biomolecule
30	Surface functionalization	MPA 1mM	The formation of linker on the AuNP
40	Activation of NHS ester	EDC 5mM NHS 2mM Mixture in MES	The carboxyl group of linker is converted to amine-reactive NHS ester
50	Immobilization of antibody	IgG type 10ug/ml	The amine group of the antibody is able to bond covalently with the linker

Table 3-1 The process flow for the surface treatment of the CNN channel to immobilize the antibody

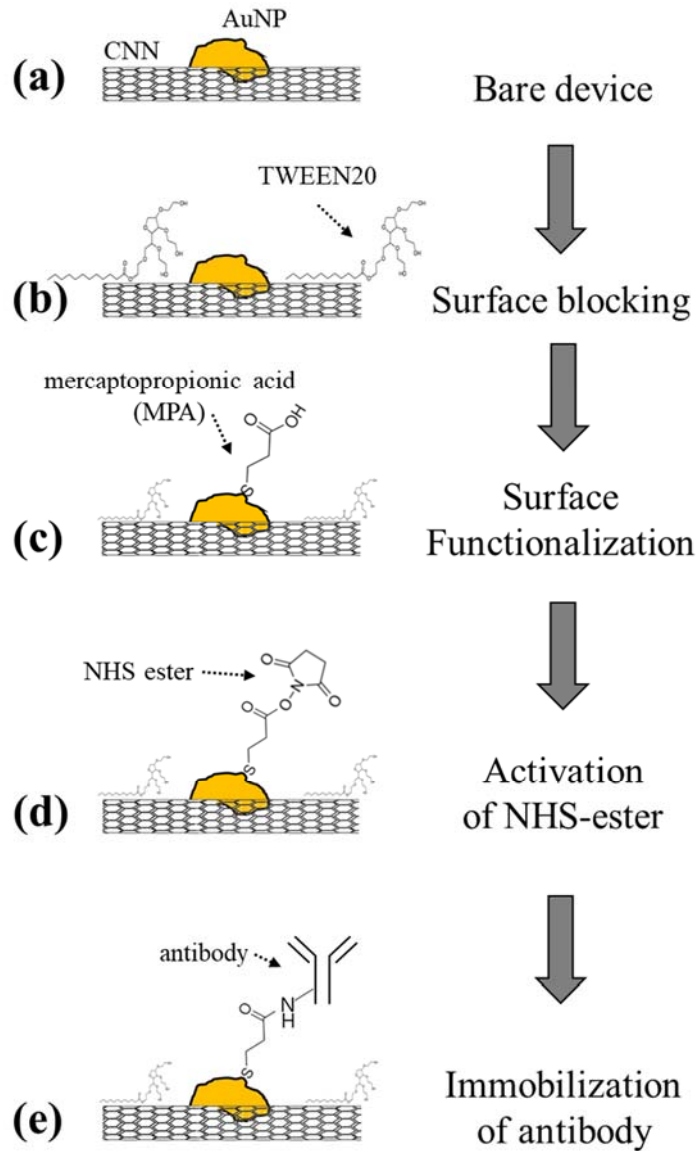


Figure 3-2 Schematic procedure of the surface treatment to immobilize antibody (a) bare device (b) the surface blocking: TWEEN20 (c) surface functionalization: MPA (d) activation of NHS ester (e) immobilization of antibody

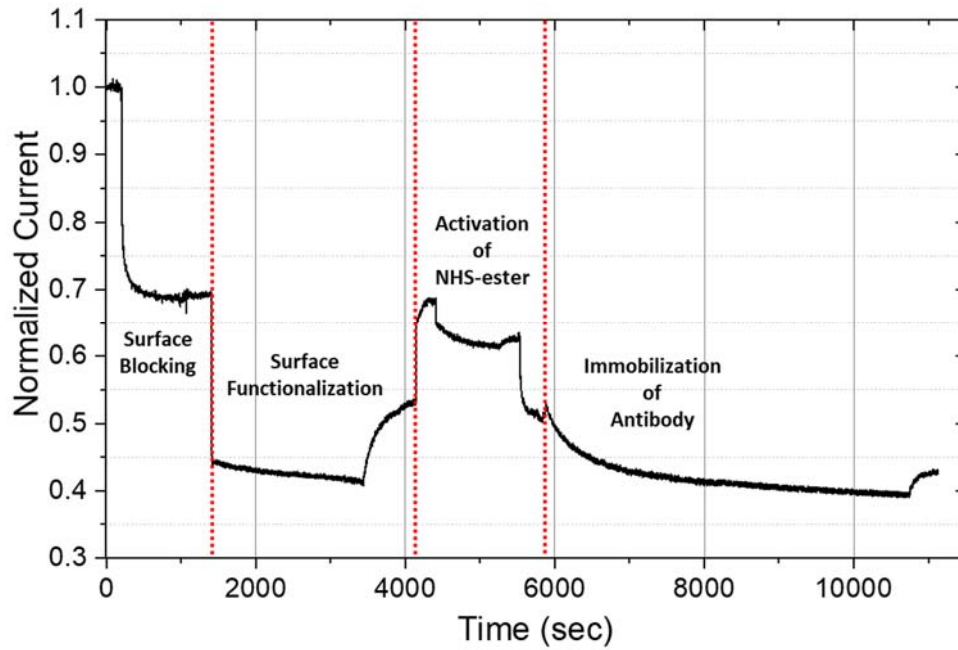


Figure 3-3 Real-time measurement of the electrical current change during the surface treatments including the surface blocking, surface functionalization, activation of NHS ester and immobilization of the antibody; all the values are normalized to the initial channel current in the PBS solution .

3.2 The electrical measurement system

To investigate the changes of electrical characteristics of the CNN channel, the modulation of the sensor device current should be obtained by the electrical measurement system. The system consists of the concentric structure device under the test, the function generator (Tektronix AFG3021), the operational amplifier (OPAMP), the oscilloscope (Tektronix DPO4104) and the power supply (Hewlett-Packard E3631A) as shown in figure 3-4.

The patterned step pulse from the function generator was applied to the drain (the island electrode) with a pulse width of a 160 μsec and the pulse amplitude from 0 V to 0.3 V for every 2 seconds. Among several types of voltage waveform, the step pulse is applied to prevent the faradaic current between the channel and the electrolyte solution. Since the faradic current degrades the channel, especially the metal surface, the magnitude and timing of the applied voltage should be carefully monitored to prevent the faradaic current.

The inverting OPAMP is used to convert the output current to the output voltage while fixing the source (the enclosing electrode) grounded through the virtual ground as shown in figure 3-5(a). The components of the output current, after the step pulse voltage is applied to the drain electrode, can be divided into two components, each having different dominance in time. The one component is dominant is the transient state after application of the unit step pulse applied,

while the other component is the steady state current after the transient state is finished (at 160 μ sec in our case), as shown in figure 3-5(c). All of the experimental results in this chapter are denoted in terms of the steady state current as the current due to the molecular binding event is dominantly modulated in the steady state current.

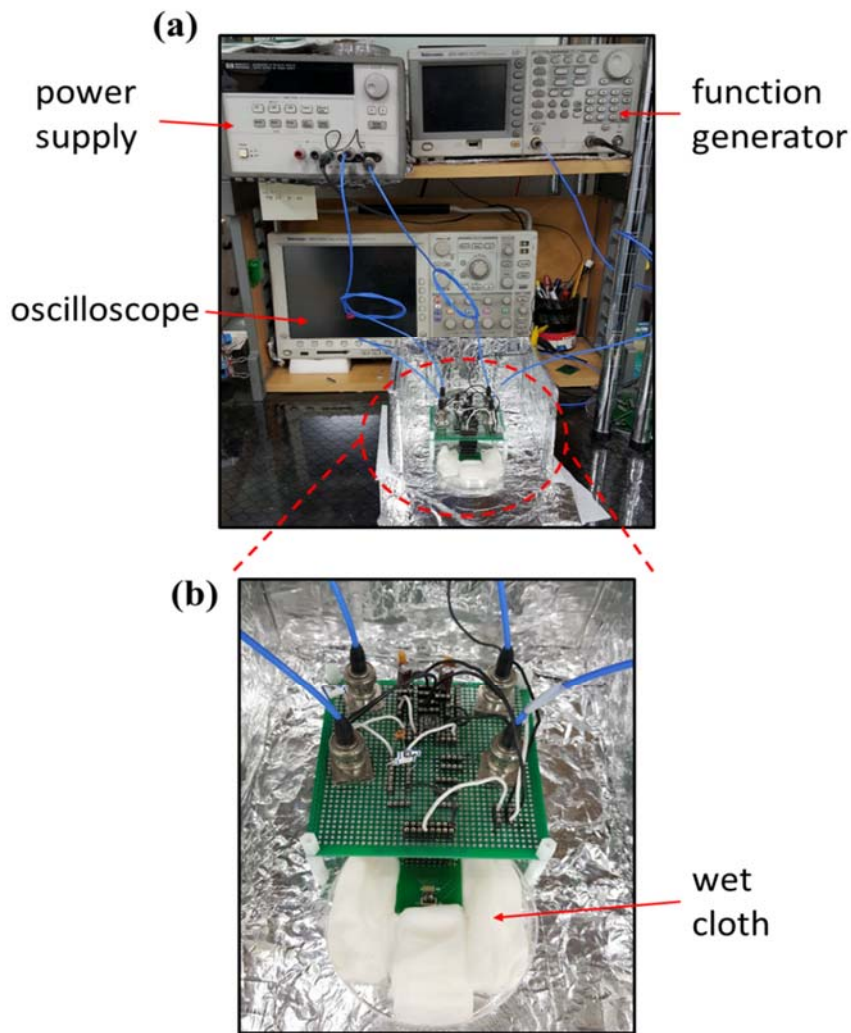
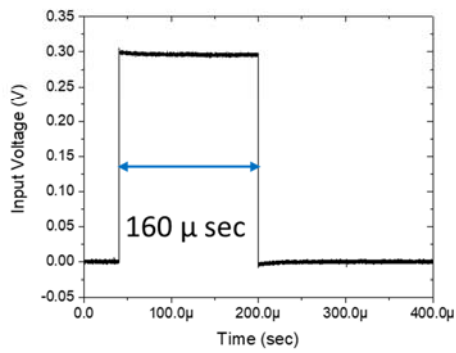
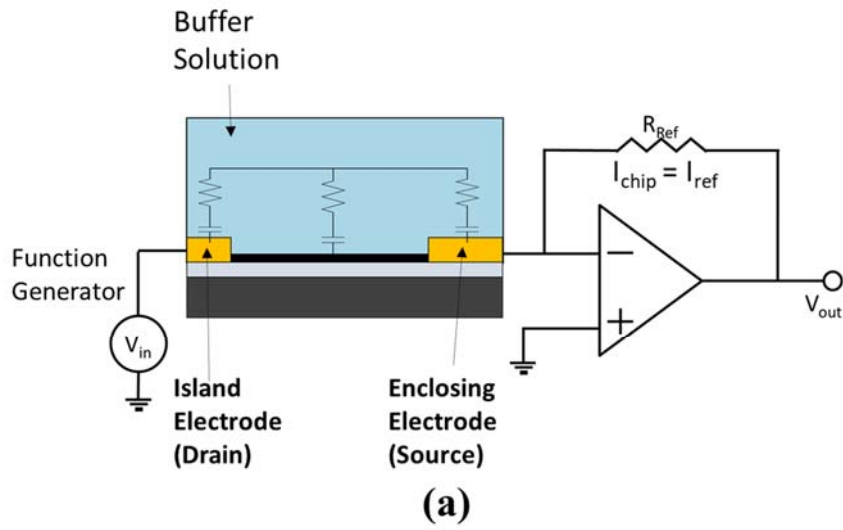
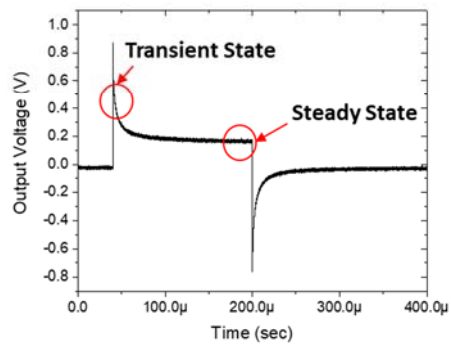


Figure 3-4 (a) The component of the electrical measurement system: power supply, function generator, oscilloscope and the circuit board with the sensor device under test.

(b) The wet cloth around the test device prevents the solution from being dried out during the measurement condition.



(b)



(c)

Figure 3-5 (a) Schematic circuit diagram of the CNN device in the buffer solution with the electrical measurement setup, (b) applied input bias voltage and (c) output voltage waveforms from the OPAMP versus time

3.3 Preparation process for the antibody immobilization

3.3.1 Surface blocking

The most of the proteins has the hydrophobicity and the electrical charge at the surface of the molecules. The surface of the CNT also has the hydrophobicity, so that the hydrophobic or the electrostatic interaction occurs between the protein molecules and the CNT, which are called the nonspecific binding [18].

The binding event of the proteins to the probe molecules of interest is called the specific binding, while binding to the other sites of the molecules is called nonspecific binding as mentioned above. The nonspecific binding on the carbon nanotubes, which is the undesirable phenomenon found with a wide range of proteins, can be overcome by introducing the polyethylene oxide chains [19]. These molecules modify the property of CNT surface to highly hydrophilic and charge-neutral, thereby eliminating the hydrophobic interactions and electrostatic binding with proteins [20].

Especially, TWEEN20, a detergent applied to forming the blocking layer to prevent the nonspecific binding, is one of the most widely used blocking layers [17]. As shown in figure 3-6, the structure of TWEEN20 consists of the two sides of different chemical properties, one with the hydrophobic and the other

is the hydrophilic characteristics. The hydrophobic side of TWEEN20 interacts with the surface of the CNT, which shows also hydrophobic property, and forms strong adsorption under irreversible chemical reaction between the hydrophobic-to-hydrophobic interactions. Therefore, after forming the blocking layer with TWEEN20, the hydrophilic side of TWEEN20 is exposed on the CNT channel surface, where the hydrophilic surface repels the nonspecific proteins from the surface of the channel region and prevents the hydrophobic interaction.

To confirm the robust formation of the TWEEN20 on the CNT surface, as shown in figure 3-7, the current response of the device in time is plotted. The PBS solution dissolved with 1% TWEEN20 was injected into the bare AuNP decorated CNN device which had been incubated in PBS. For 15 minutes, as reported in other papers [21], the current slightly decreased during Tween-20 treatment and never increased back to the original level even after washing the device. From the observation, the irreversible reaction between the TWEEN20 and the CNT surface can be confirmed.

In addition, by observing the decreasing current response during the reaction time, the formation of the TWEEN20 on the CNT surface was electrically observed. To test the biochemical validity of the blocking layer of TWEEN20, the solution with a high concentration of the nonspecific protein was injected

on purpose and the current response of the sensor device was measured. The bovine serum albumin (BSA) was chosen as the nonspecific protein with the concentration of 10 mg/ml. Two devices group were prepared. The one was treated with the TWEEN20 as the surface blocking and the other was a control without the surface blocking layer in comparison to the surface-blocked device. From the drastic change in the current from the surface-blocked device was observed, it can be concluded that the nonspecific protein adsorption on the CNT surface is largely depressed by the TWEEN20 blocking layer.

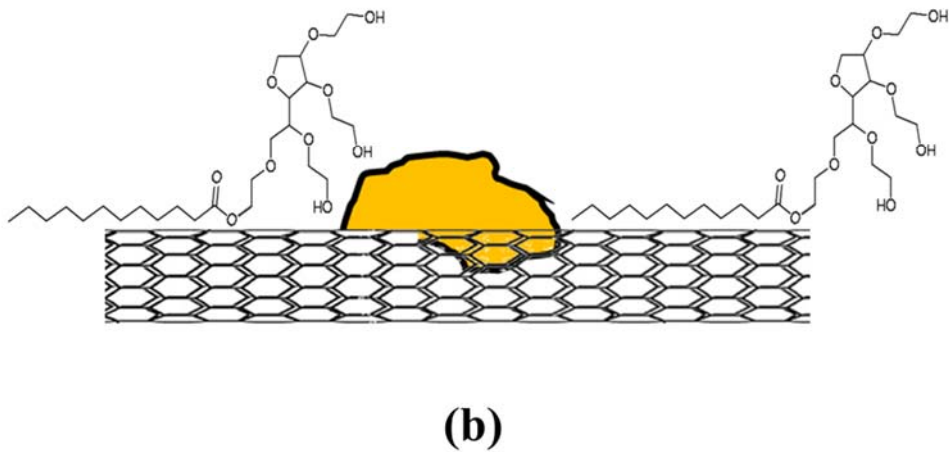
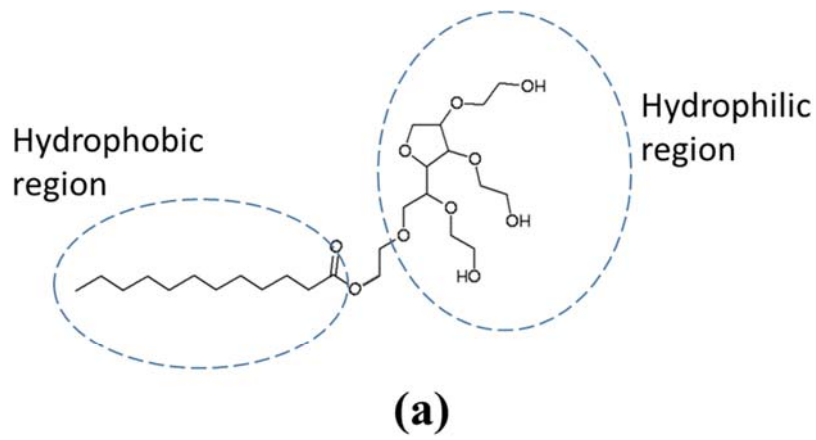


Figure 3-6 (a) Structure of the TWEEN20 consists of the hydrophilic and hydrophobic region. (b) Schematic illustration of the TWEEN20 adsorbed to the CNT surface forming the blocking layer.

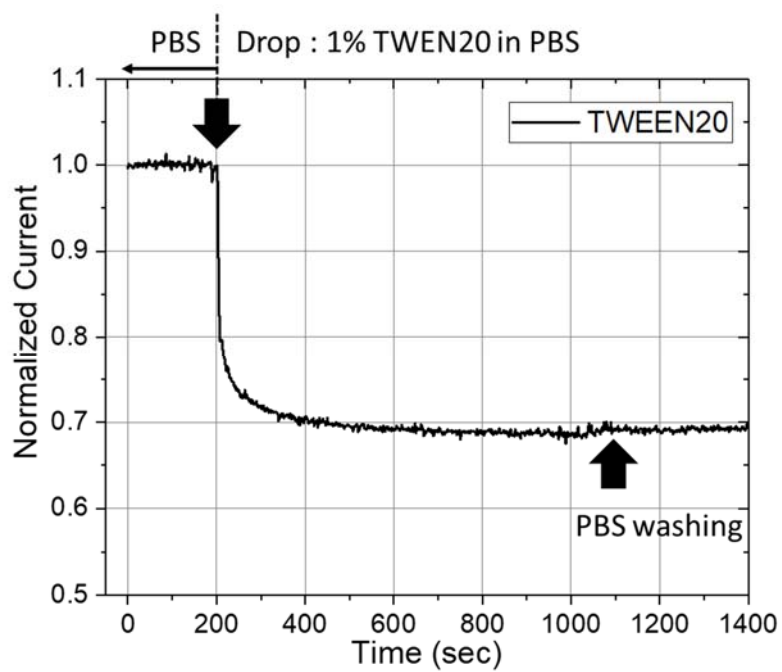
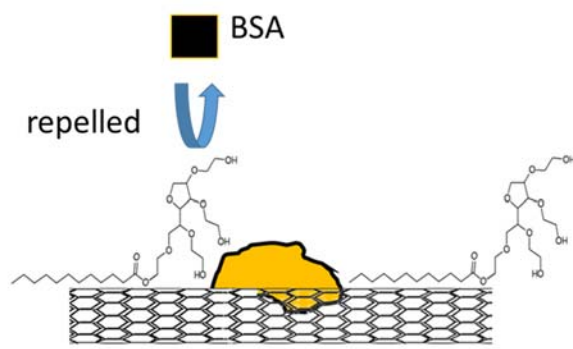
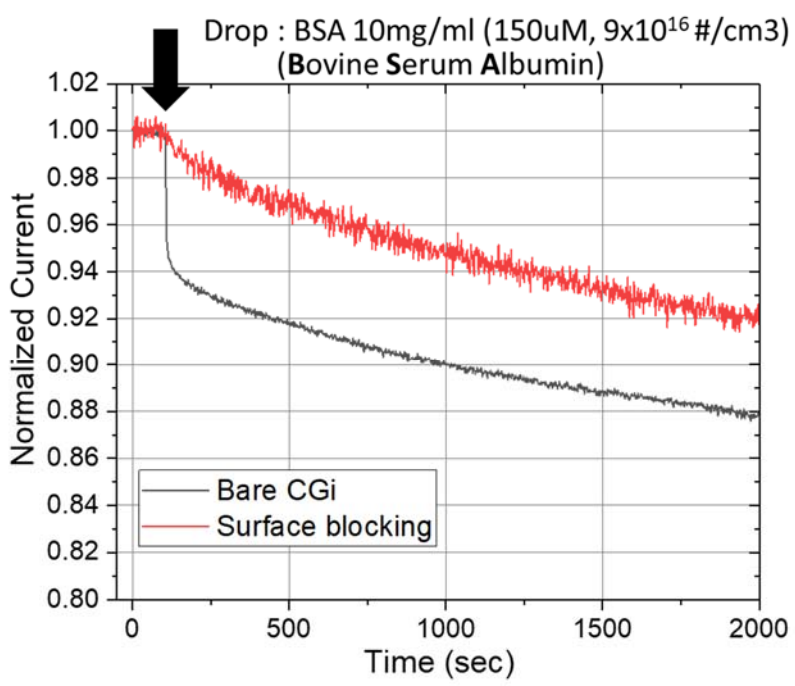


Figure 3-7 Real-time measurement of current change during the surface blocking with 1% TWEEN20 in PBS



(a)



(b)

Figure 3-8 (a) Schematic of a monolayer of TWEEN20 adsorbed on a nanotube, repelling nonspecific binding of proteins in solution. (b) Real-time measurement of sensor current during adsorption of the BSA; the bare device (black line), the device with the TWEEN20 (red line)

3.3.2 Surface functionalization

The MPA molecules have been used as the interlayer to attach the antibody to the gold surface. The MPA contains a carboxyl group at one end and thiol group at the other end, as shown figure 3-9(a).

Proteins can bind to the gold nanoparticle (AuNP) through several types of interactions such as electrostatic interaction, hydrophobic interaction and dative bond [22]. Despite its and convenient formation of antibody on the AuNP with above-mentioned interactions, the immobilized antibody cannot be arranged with the certain orientation, which affects the binding rate between the antibody and the antigen reaction [23]. The orientation of the antibody can be controlled by introducing the linker molecules [24]. MPA is chosen as the linker molecule, which connect the link between the AuNP and the antibody providing the antibody with the orientation to enhance the binding rate to the target molecules. The AuNP surface is modified with 3-mercaptopropionic acid (MPA) for 30 minutes where the other surface region of the CNT channel except for the AuNP region was blocked with the TWEEN20. The MPA formation was confirmed by observing the electrical current response of the device after injecting the MPA solution into the channel of the device. Once the 1 mM of MPA solution was injected into the device, the current rapidly decreases. During the washing procedure with PBS, the decreased current

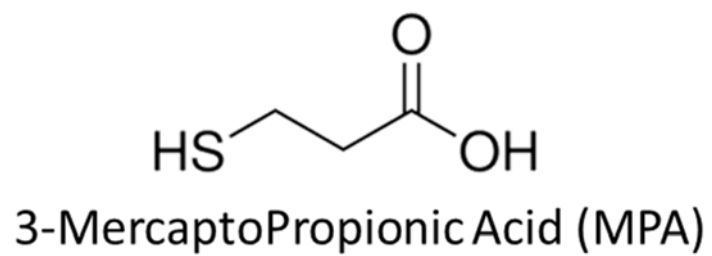
increases again.

Here, the cause of the current change during the surface modification of the channel is observed in figure 3-10. The chemical bond formation between MPA and AuNP causes the work function of AuNP to decrease. Since the decrease in the work function of the AuNP changes the band structure of the device channel to deplete the concentration of the holes, which are the majority carrier of the CNT, the current decreases. The decreased current recovers back during the washing procedure because the desorption of the unstably bonded MPA increases the hole concentration of the CNT surface.

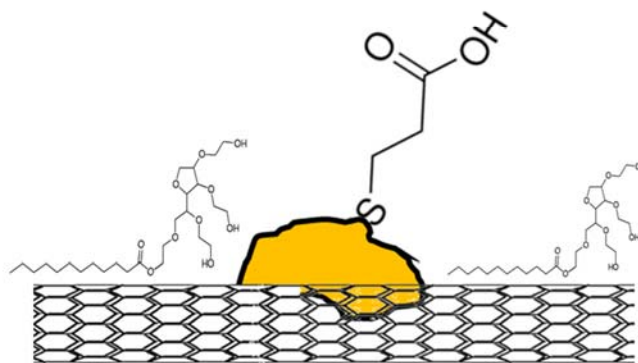
To confirm whether the MPA is bonded onto the AuNP surface or not, as a control experiment, the MPA solution was injected into the CNN device without the AuNP.

After washing step, the CNN device without the AuNP recovers the current characteristics to its original level, while the AuNP decorated CNN device recovers the current characteristics only to its 25% of the original level. It should be noted that there is no site for the MPA to form the chemical bond in the case of the CNN device without the AuNP.

From the result, we can confirm that the MPA is stably formed on AuNP surface of the device even after washing treatment.

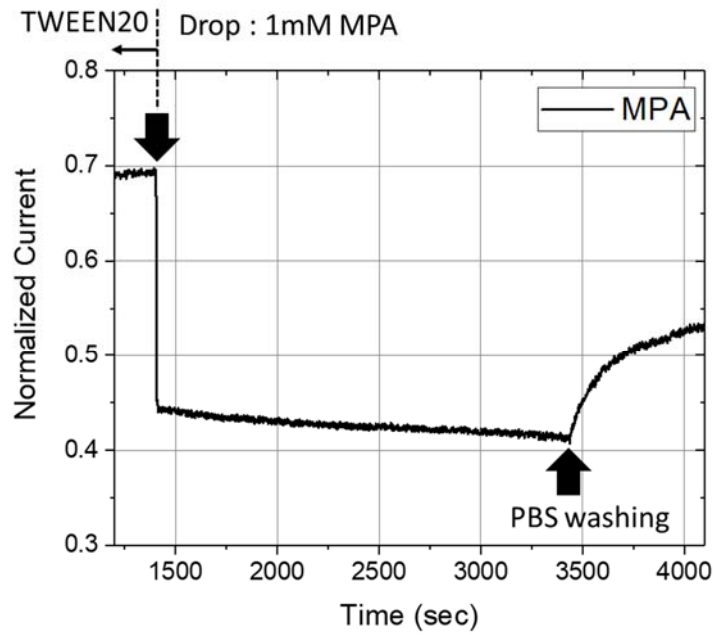


(a)

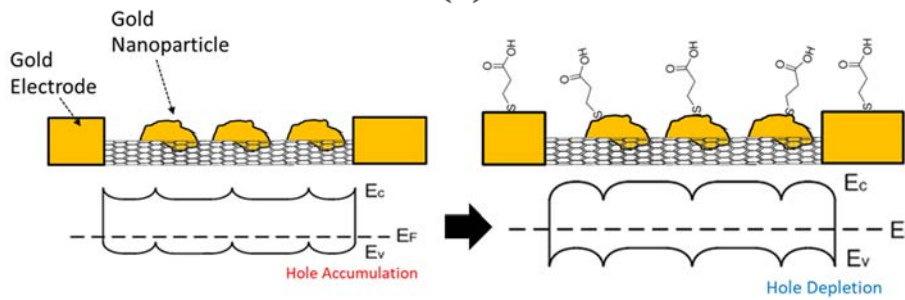


(b)

Figure 3-9 (a) Structure of MPA (b) Schematic illustration of device surface modified with MPA

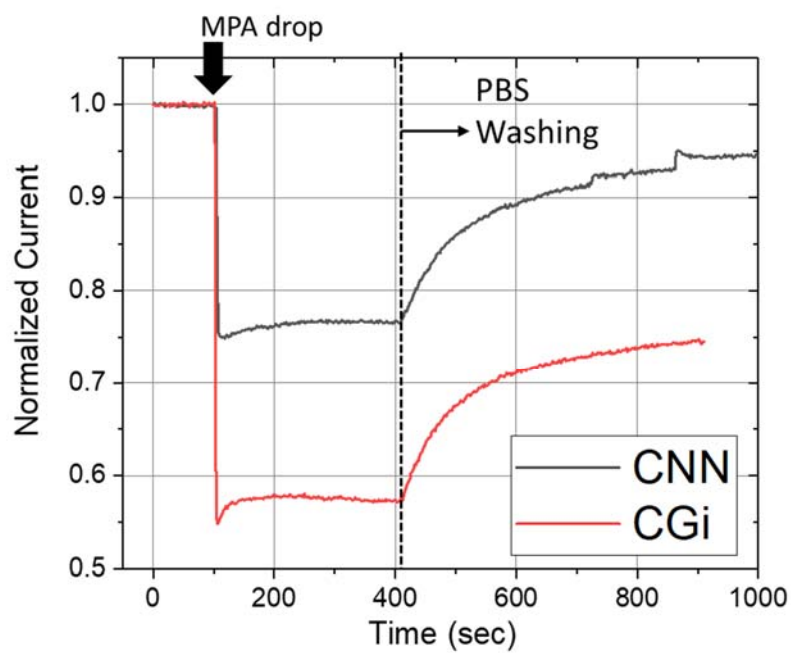


(a)

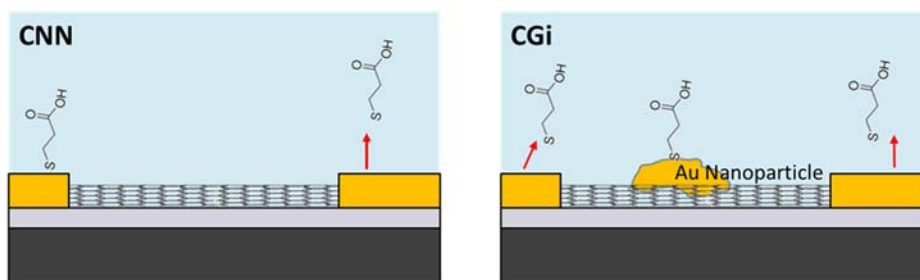


(b)

Figure 3-10 (a) Real time measurement of current change during MPA adsorption and washing process (b) Energy band diagram of the device; The current decreases after binding the MPA on the surface since the thiol-molecules reduce the work function of gold.



(a)



(b)

(c)

Figure 3-11 (a) Real time measurement of current change during the MPA adsorption and washing process. Schematic illustration of the device structure with MPA on (b) the CNN device without the AuNP, (c) the AuNP decorated CNN device

3.3.3 Activation of the NHS-ester

The mixture of the EDC and NHS is applied to activate of the carboxyl group in the MPA, which has been attached on the AuNP. EDC has been used to activate the carboxyl group for coupling biomolecules [25]. EDC is a water soluble carbodiimide cross-linker and is widely used to couple the carboxyl group with the amine group of the protein molecules. EDC reacts with a carboxyl of the MPA to form an amine-reactive O-acylisourea intermediate. EDC couples NHS to carboxyls, forming an NHS ester that is considerably more stable than the O-acylisourea intermediate. Thus, the amine group of the protein can be linked to the NHS ester by the covalent bonding [26]. Because the reaction of EDC is most efficient in the acidic conditions and must be performed in buffers with amines, the MES buffer (4-morpholinoethanesulfonic acid) has been used as a suitable carbodiimide reaction buffer [27].

The initial condition of the MPA modified on the AuNP is the PBS solution (pH 7.4). For the EDC/NHS reaction, the reaction environment condition is changed to the MES buffer solution (pH 4.7). The device surface is reacted with the EDC/NHS mixture solution. Finally, to immobilize the antibody by substituting the antibody for the NHS ester, the buffer condition is changed again to the PBS. (See figure 3-12(b))

Once the buffer solution is changed from the PBS to the MES condition, the current rapidly increases as the MES buffer solution has the lower pH value than PBS and the current of the CNN device is enhanced under low pH value at the same bias condition as reported previously [5]. To demonstrate the pH dependence of the device behavior, the current change was measured with the MPA modification in the various pH solution as shown in figure 3-13.

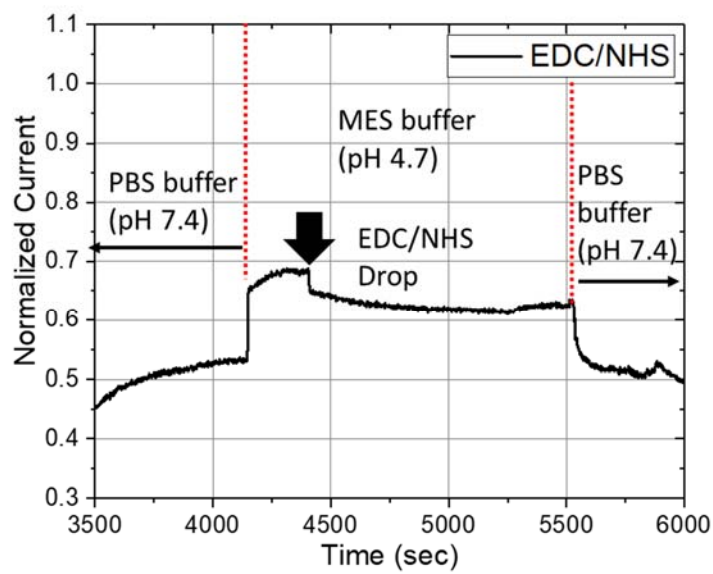
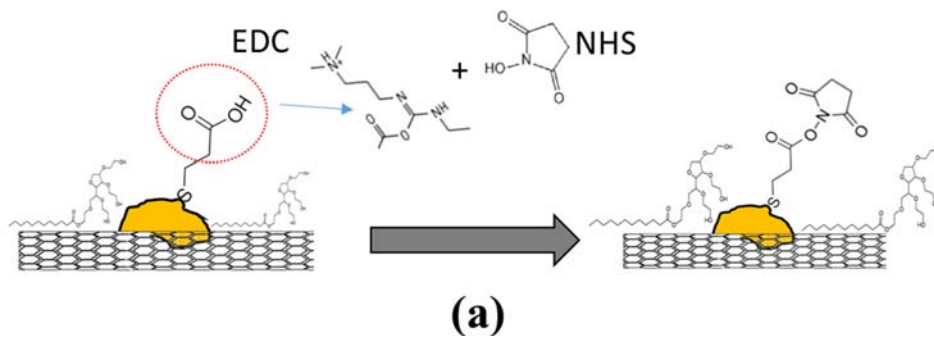


Figure 3-12 (a) Schematic illustration of the MPA being converted to NHS ester by the reaction of EDC (b) Real time measurement of the current change during the EDC/NHS reaction

$$\text{Rate of Current Change} = \frac{I_{pH\#} - I_{PBS}}{I_{PBS}}$$

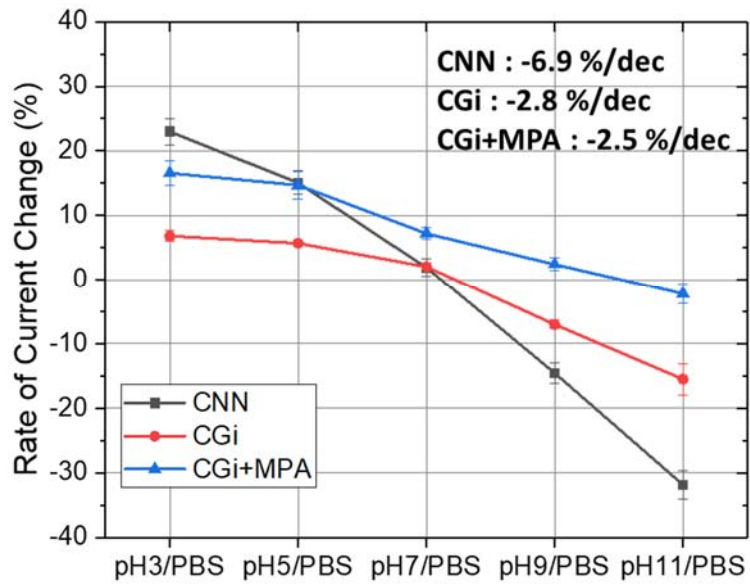
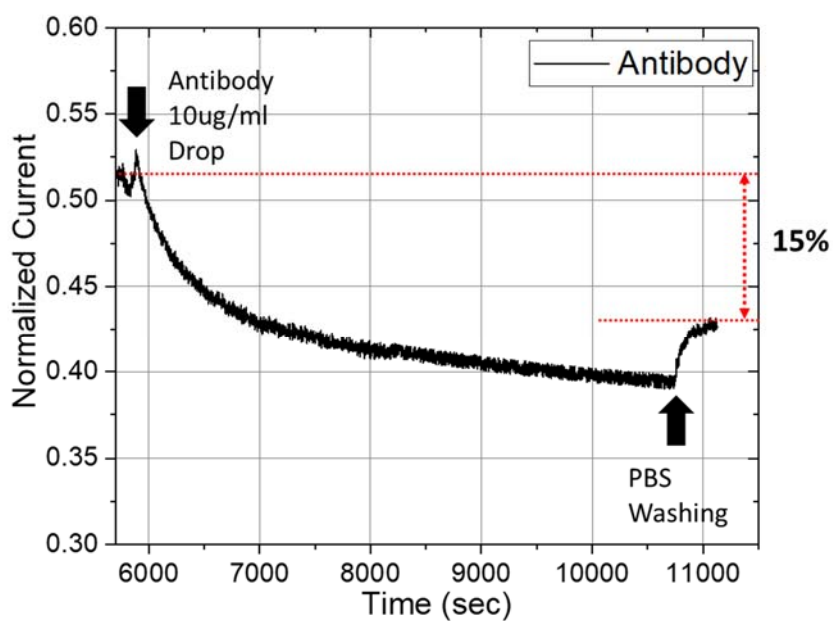
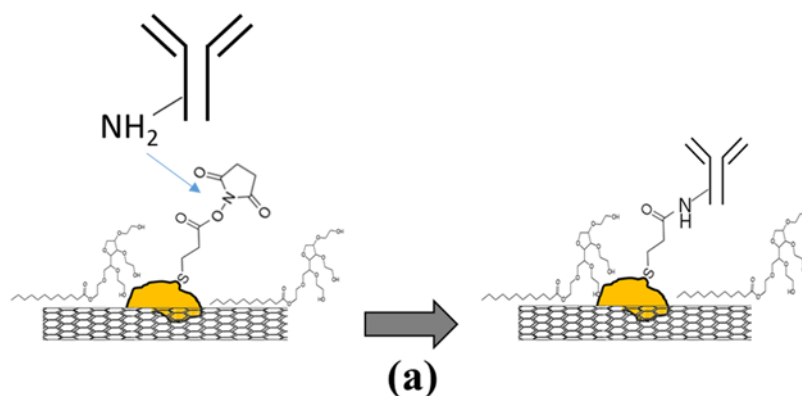


Figure 3-13 pH dependence of the channel current for various device structures; the CNN device (black), the AuNP decorated CNN device (red) and the MPA on the AuNP (blue)

3.3.4 Immobilization of the antibody

Now, the NHS ester group at the end of the MPA linker molecule is substituted for its original carboxyl group. For antibody immobilization, the NHS ester site is reacted with the IgG-type antibody with the concentration of 10 ug/ml for 1 hour and 30 minutes. The amine group of the antibody can be linked to the NHS ester on the AuNP by the covalent bonding. The electrical current decreases about 15% quite consistently for many device samples used in this work, implying that the surface treatment is quite reliable as shown in figure 3-14(b). The figure 3-14 shows the decreasing and increasing response of the current characteristics. The decreasing current region is due to the immobilization of the antibody on the NHS site of MPA linker molecule while the increasing current region indicates the desorption of the antibody from the unstably bound state on the channel surface during the washing procedure. As mentioned above, the antibody has been immobilized on the device channel surface utilizing the combination steps of the surface blocking, MPA linker, EDC/NHS reaction and amine group of the antibody molecule. The method can be considered as the procedure for the general biosensor platforms having the AuNP as the channel element. Every kinds of the biomolecules, especially antibodies with amine group at the surface can be immobilized on the AuNP surface of the biosensor device.



(b)

Figure 3-14 (a) The amine group of the antibody can be linked to the NHS ester on the gold nanoparticle. (b) Real time measurement of current change during the antibody immobilization on the NHS ester site at the MPA linker molecule

3.4 Experiment results for the antibody-antigen reaction

In the order to test the feasibility of the platform explained in the previous section, the α -fetoprotein (AFP) as the target molecule is adopted. AFP is a major plasma protein produced by the yolk sac and the liver during fetal development. Clinically, AFP is known as the biomarker of hepatoma of the adults [16]. The concentration of AFP in the human blood is over 1 ug/mL in the case of the patient group at risk of the hepatoma while it remains under 15 ng/mL in the case of the normal. If the biosensor device can detect and distinguish the concentration of AFP around 1 ug/mL, it can be used for the diagnosis of the hepatocellular carcinoma (cancer).

The current change of two sensor devices, one for the probe-target binding reaction and the other for the control experiment for the nonspecific binding effect, was measured during 20 minutes after injecting the AFP as the specific target molecule and BSA as the nonspecific control molecule with the same concentration of 10 ug/mL in the PBS buffer solution. The molecular concentration of 10 ug/mL used in this experiment is 10 times higher than the cut-off level of the hepatocellular carcinoma.

To compare with the control experiment, the device with the AFP target molecule shows an appreciable change in the current response. About 5% of the current change in the case of the probe-target experiment is obtained while

about 2% of that is obtained in the case of the control experiment. Since the more current change was observed in the case of the device with the AFP than in the case of the control device, the result confirms the antibody of the AFP is properly immobilized as the prober molecules on the device surface shown in figure 3-15.

Next, the experiment to investigate the performance (dynamic range) of the sensor device was performed. The concentration of the AFP and the BSA in PBS buffer solution are varied to see the response of the sensor to the specific and nonspecific molecules. The current responses were measured for both AFP and BSA cases with the concentration of 0.1 ug/ml, 1 ug/ml and 10 ug/ml. Additionally, other control experiments were conducted in the case of the pristine PBS without any proteins and the undiluted human serum containing concentration of the various kinds of nonspecific proteins.

As shown in figure 3-16, for all occasions, the lower concentration of the proteins are injected, the less current variations are observed from the sensor devices. The highest current change is obtained at the highest concentration of 10 ug/ml. However, under the cut-off level of 1 ug/ml, there are no appreciable current change in comparison with the control experiment for only the BSA.

Since the negligible change in the current is observed in the case of the pristine PBS without any proteins, it is convinced that the sensor device shows

a stable reliability.

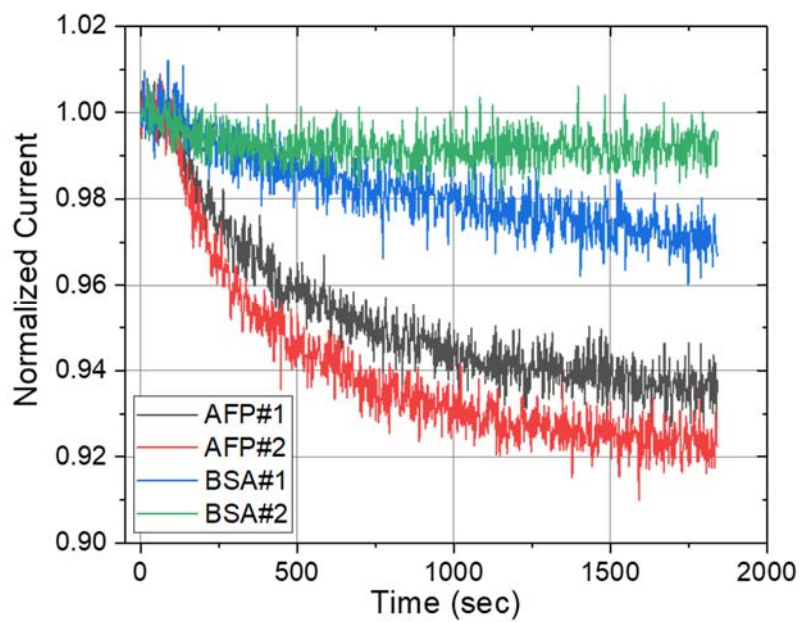
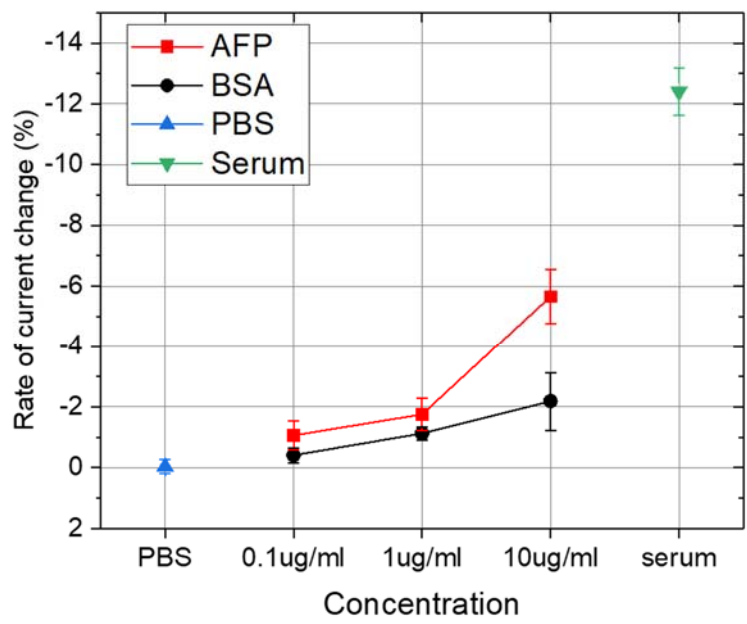


Figure 3-15 Real time measurement of current change during the specific binding (AFP) and nonspecific binding (BSA) events.



PBS	Mean	S.D	AFP	Mean	S.D	BSA	Mean	S.D
	-0.039	0.231	0.1ug/ml	-1.064	0.460	0.1ug/ml	-0.408	0.236
Serum	Mean	S.D	1ug/ml	-1.757	0.541	1ug/ml	-1.133	0.214
			10ug/ml	-5.660	0.884	10ug/ml	-2.188	0.950

Figure 3-16 The rate of current changes for various concentrations of specific and nonspecific molecules. The data for the PBS and serum conditions are also shown.

3.5 Conclusion of chapter 3

To detect the target proteins, the sensor platform with the AuNP decorated CNN between the concentric electrode structure was developed. To immobilize the antibody of the target protein as the probe molecule the chemical treatment was carried out on the channel surface of the device. In a number of the devices, this chemical treatment was performed by showing stable and reproducible results.

In order to check that the antibody was immobilized on AuNP surface with the proper orientation, the reaction experiments for the probe antibody-target AFP binding and the control experiment were performed. In the case of the high concentration (10 ug/ml) of the target proteins, the appreciable amount of the change has been observed where the difference between the specific target molecule AFP and the nonspecific protein BSA can be observed. However, under the cut-off level of the concentration of the target proteins, it was hard to recognize the difference between the specific and nonspecific binding events. For a successful biosensor application, the device should distinguish the concentration of the target molecule under the cut-off concentration in the human blood or the serum conditions.

Unfortunately in the result of the experiments using our sensor devices, the current change due to the serum caused by the nonspecific molecules surpass

the change of the sensor caused by the target protein under the cut-off concentration. The device in this level of the performance cannot be used as a practical biosensor application. Therefore it should be found that a special method to enhance the sensitivity of the device to the specific interaction between the target and the probe proteins.

Chapter 4

Strategy for enhancement of sensor performance

In the developed sensor platform, the current change occurs because of the specific binding interaction between the antibody and the antigen. However, as seen in the previous chapter, the current change was not sufficiently large to detect the target molecule and distinguish the target from the nonspecific molecules. To overcome the problem and enhance the performance of the sensor device, the electrical and the chemical methods are suggested in this chapter.

The electrical method facilitates the previously mentioned protocol of the surface treatment as it is. This method is based on the physical property of the device to enhance the change of the current response. There can be two techniques expected to be used electrically to enhance the change of the current response. These techniques were developed by using the device introduced in this dissertation and have been previously reported [7][8].

There also exist two chemical techniques to enhance the change of the current response. One is to change the linker molecule used in the previous surface treatment. And the other is to insert additional chemical treatment during the sensor device preparation.

4.1 Transient measurement

In high ionic strength solutions, the charge of the target molecules is screened by many counter ions in the solution and therefore the electrical field of the biomolecules cannot affect on the current of the channel. In order to overcome this problem, a simple electrical sensing method was suggested, which is called as a transient measurement method [7]. The electrical current is measured after the step voltage is applied between the channel and the electrolyte solution. In initial steady state, both the CNN channel surface and the charged target molecule are screened by the counter ions. The counter ions are swept away by high external electric field and the charged molecules efficiently give effect to the surface of the channel until the screening ions are redistributed as shown in figure 4-1.

Since the output current, when the pulse bias is applied, consists of both the capacitive current through the electrolyte solution and the channel current through the CNN, it is necessary to separate the channel current from output current in order to observe the change of the channel conductance. The channel current can be calculated by subtracting the capacitive discharging current from the charging current. As shown in figure 4-2(c), the transient current is defined as the moment channel current when the step pulse is applied.

The change of the transient current obtained by the previously mentioned

method is compared with that of the steady state current. Three cases of the devices were prepared: 1) the pristine PBS without any proteins, 2) AFP protein dissolved PBS, and 3) the BSA dissolved PBS as a nonspecific control. The concentration of AFP and BSA was 1 ug/ml which is the cut-off level of the hepatocellular carcinoma.

As seen in figure 4-3, there exists negligible current change between the transient state and the steady state. Since the size of the antibody is relatively large (about 10 nm) compared with the Debye length, a number of counter ions being swept away and de-screen the charge of the antigen under the electrical bias condition may be negligible. It should be noted that the success of the transient measurement method applied to the DNA sensing may be ineffective in the antibody-antigen reaction.

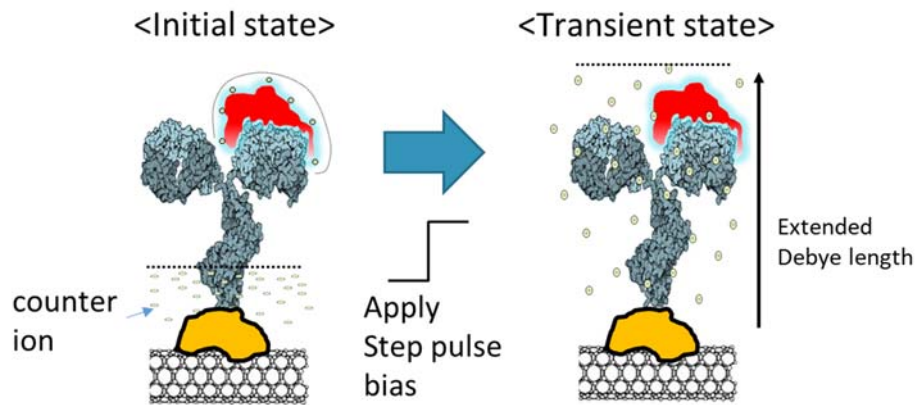


Figure 4-1 Schematic illustration of transient measurement method; There exists a space charge layer at the interface between the solution and the protein, which screens the electrostatic field induced from the charged molecule over the Debye length. After the step-pulse bias, the Debye length is extended instantaneously, the screening counter-ions around the target molecule are swept away during the transient state.

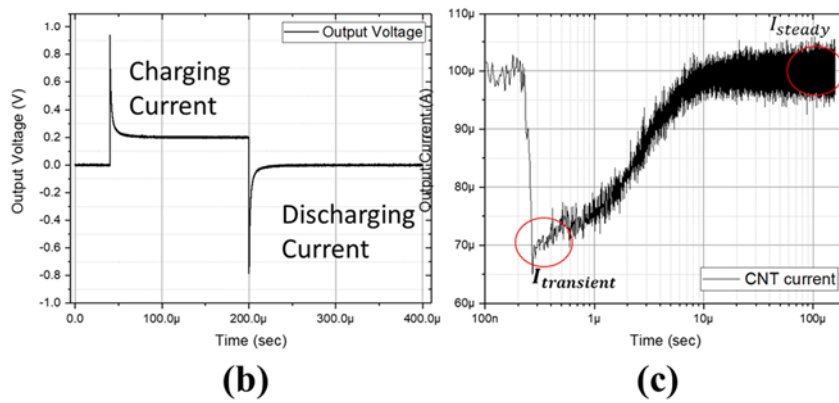
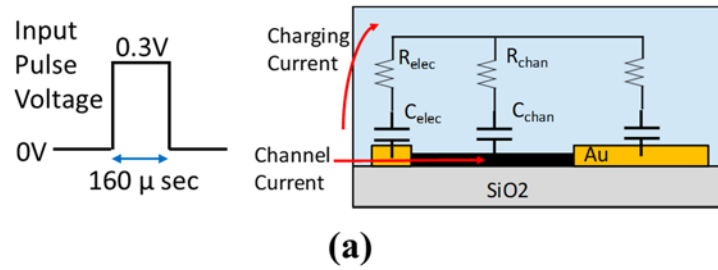


Figure 4-2 (a) schematic diagram of current component of the device in the solution (b) the output voltage when the step pulse is applied; (c) the channel current; the CNT current can be calculated by subtracting the discharging current from the charging current

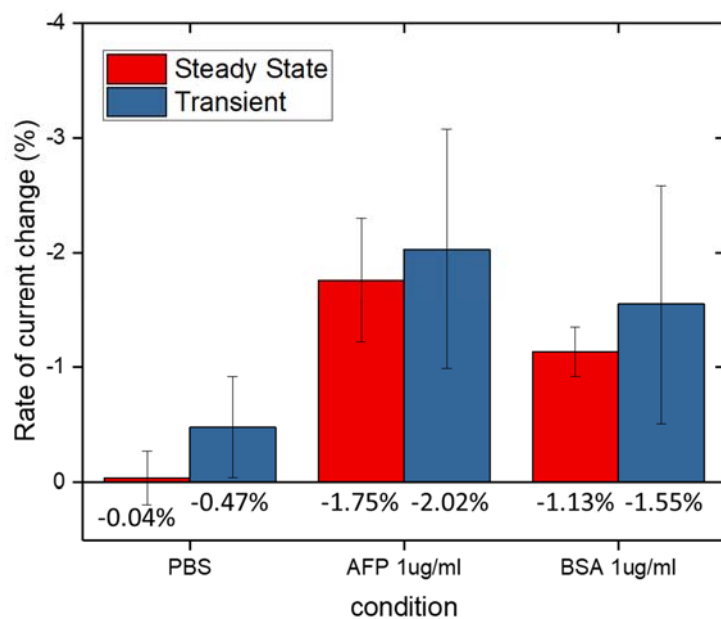


Figure 4-3 Comparison of the current change between the transient state and the steady state; the difference between steady state current and the transient state current is negligible for the cut-off concentration of AFP (1ug/ml).

4.2 Enhancing the specific binding event: ACEF (AC Electrothermal Flow)

The alternating current (AC) electrokinetic is one of the most promising techniques used to enhance a binding reaction between the probe molecules and the target molecules [28]–[31]. The AC electrokinetics can be categorized into three kinds such as the AC electrothermal flow (ACEF), AC electro-osmosis (ACEO), and dielectrophoresis (DEP). Among them, the ACEF is suitable for biosensors as it can effectively operate in highly conductive biological media (about 1 S/m). When the non-uniform electric field is applied, locally changed temperature by the Joule heating induces the gradient of the permittivity and conductivity of the solution. Due to the effect of these gradients, the molecules in the solution is circulated by the induced electrothermal flow. Therefore, the AC bias to the electrode induces circulation of the solution flow, which facilitates the transport of the target molecules to the binding region

From previous studies from our group [8], it has been shown the ACEF on the AuNP decorated CNN device can significantly increase the sensitivity and specificity of the biosensor assay for detecting the cardiac troponin I (cTnI) which is a specific cardiac biomarker for the diagnosis of acute myocardial infarction. Because the appreciable current change was observed by using the

ACEF method in the previous experiment, the ACEF method is introduced in our antigen-antibody reaction experiment. The molecular concentration of the experiment is same with that in section 4.1 during the reaction of the antigen and antibody, and ± 5 V amplitude of the voltage was applied to the drain electrode with 1 MHz frequency. After the reaction for 20 minutes, the current change was compared. As shown in figure 4-4, the channel current decreases when the ACEF method is applied to the device only with the immobilized antibody. On the other hand, there is no significant current change in the steady state current with and without the antibody protein.

Inefficiency of the ACEF method in our device may be speculated as; after the ACEF method is applied, the temperature nearby the electrode and the channel surface increases. As the protein can be denaturalized in the high temperature [32], the affinity of the antibody immobilized on the channel region decreases. The quantitative understanding of the inefficiency of the ACEF should be the subject of the further study.

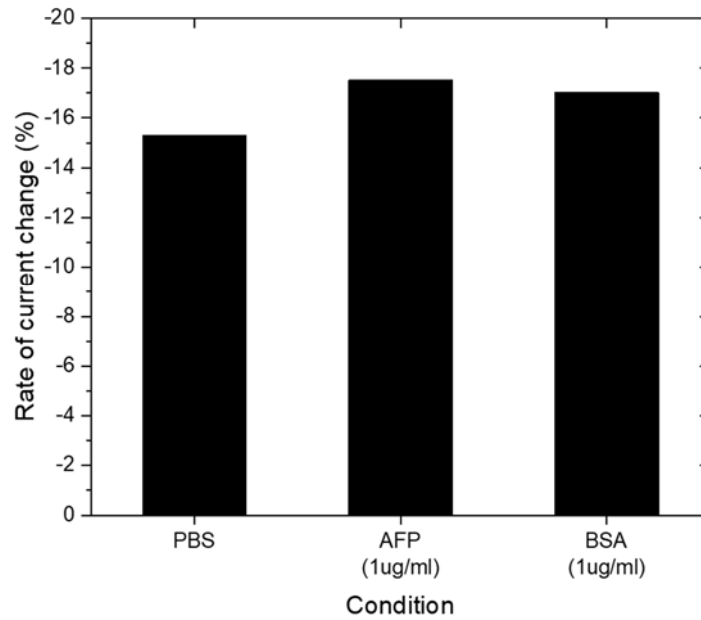


Figure 4-4 The rate of current changes when the ACEF method is applied for various conditions; there is no difference in the current change between specific binding and nonspecific binding. High temperature caused by the ACEF may lead to degradation of the binding efficiency due to deformation of the antibody proteins.

4.3 Introduction of linker

Various self assembled monolayers (SAM) of the n-alkanethiols of different chain lengths deposited on the gold surface have been used to immobilize antibody [33][34]. As described in chapter 3, the MPA linker with the shortest molecular chain length among the n-alkanethiols was chosen to form the antibody-immobilization site close to the AuNP surface. However, the various researches using the SAM layer report that the antigen-antibody binding efficiency called the affinity of the antibody can be changed by the different molecular chain length of the alkanethiol as the linker molecule [35].

In this work, the 11-mercaptoundecanoic acid (MUA) was chosen as a linker molecule for the antibody as the molecule has been reported to give the best binding efficiency for the antigen to the antibody [24]. Once the antibody was immobilized on the AuNP surface, the molecular chain length of the n-alkanethiol is known to determine the orientation of the antibody. The longer chain length is selected, the more epitope of the antibody can be exposed to the solution, thereby the binding efficiency with the antigen molecule can be enhanced. The shorter the chain length is selected, the less epitope of the antibody can be exposed out. The binding efficiency with the antigen molecule can be diminished in this case.

As the third method, to enhance the performance of our sensor performance,

the MUA linker was substituted for the MPA linker and the antigen-to-antibody reaction with AFP was tested. As shown in Fig 4-5, the only the linker molecules were changed while other conditions and surface treatment were kept same as the previous experiments.

The current response was observed for the device with the MUA linker after injection of the AFP antibody of 10 ug/ml.

As shown in Fig 4-6(b), the MUA device shows faster current change compared with the MPA device. The amount of the current change in the case of the MUA is less than that in the case of MPA. It may be understood that longer molecular chain of MUA enhances the binding efficiency of the antibody thereby showing fast response in current. However, the distance between the channel surface and the antibody (epitope) due to longer MUA, increases and the final current change may not be improved while the binding efficiency may be increased.

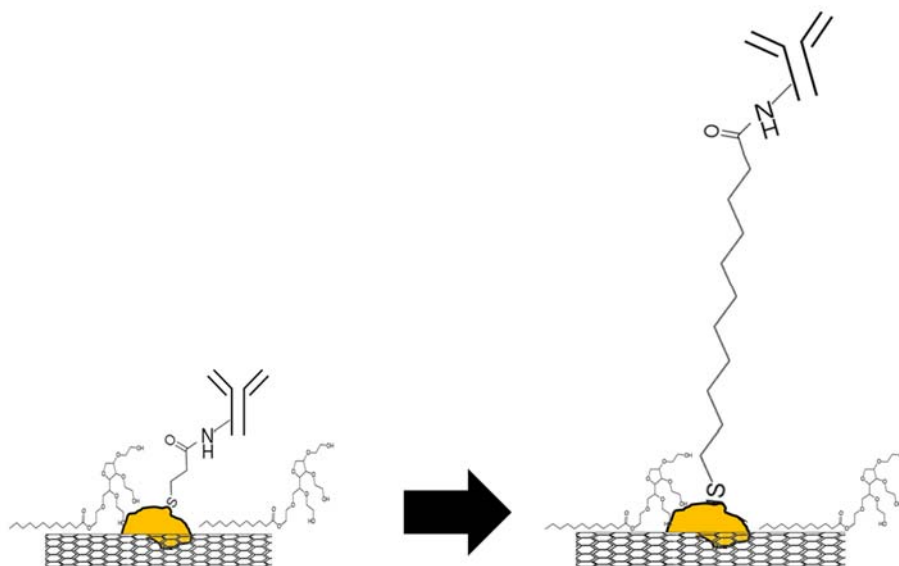


Figure 4-5 Schematic illustration of the effects of the linker materials; the MUA linker was substituted for the MPA linker to immobilize the antibody on the channel surface.

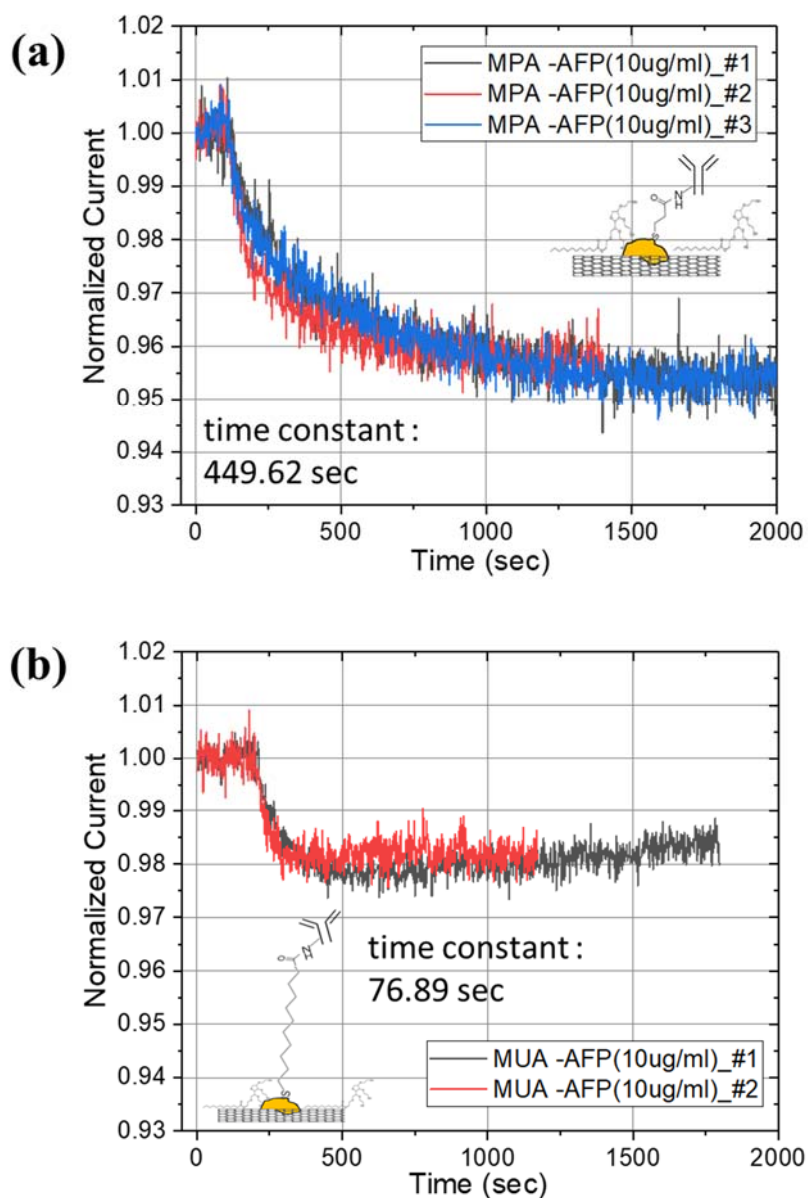


Figure 4-6 Real time measurement of the current change during the reaction between the antibody and the 10 ug/ml of antigen AFP (a) MPA as a linker (b) MUA as a linker

4.4 NHS-ester deactivation

As the final strategy to enhance the sensor performance, deactivation of the NHS-ester unbound with the antibody has been performed. As explained in the section 3.3, the amine group in the antibody reacts with the NHS ester. After immobilizing the antibody on the channel surface, there still exists the NHS ester sites yet to be reacted with the antibody. In this situation, if the target molecule is injected, the target molecule may react with the NHS ester sites not with the antibody [36]. Therefore, the effective concentration of the target molecule, which reacts with the antibody, can be underestimated due to the unwanted NHS-target protein reaction. In the conventional researches, to deactivate the remaining NHS ester, the chemical material with the amine group (i.e. hydroxylamine, Tris, or glycine) has been used to deactivate the unbound NHS-ester [37]. In this work, the remaining NHS esters after immobilization of antibody are deactivated with the BSA which have the amine group as shown in figure 4-7. A test device has been prepared after immobilizing the antibody on the device surface and deactivating the NHS ester sites with BSA, and the experiment was carried out with the AFP (specific) and BSA (nonspecific) of 10 ug/ml as the target molecules.

As shown in Fig 4-8, there is no significant change in the current response in case of the nonspecific protein BSA injection. In the case of the specific

target, AFP, the change in the current response is also decreased, which is undesirable (rate of current change decrease shown in figure 3-15 in section 3.4)

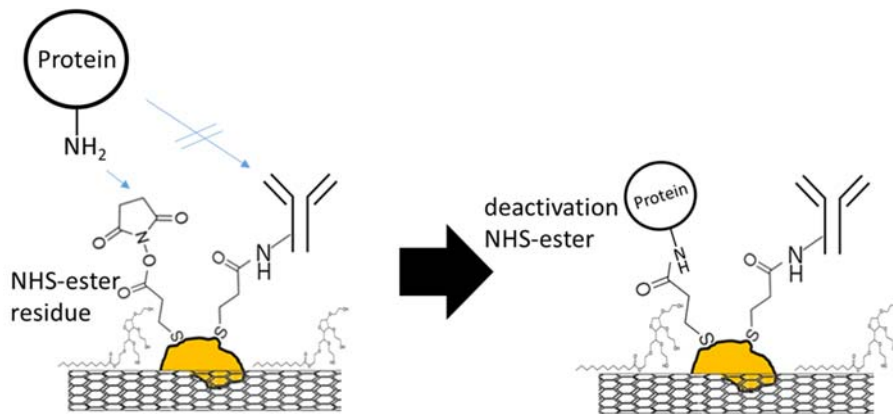


Figure 4-7 Schematic illustration of the deactivation procedure; The remaining NHS esters after immobilization of antibody are deactivated with other proteins which have amine group

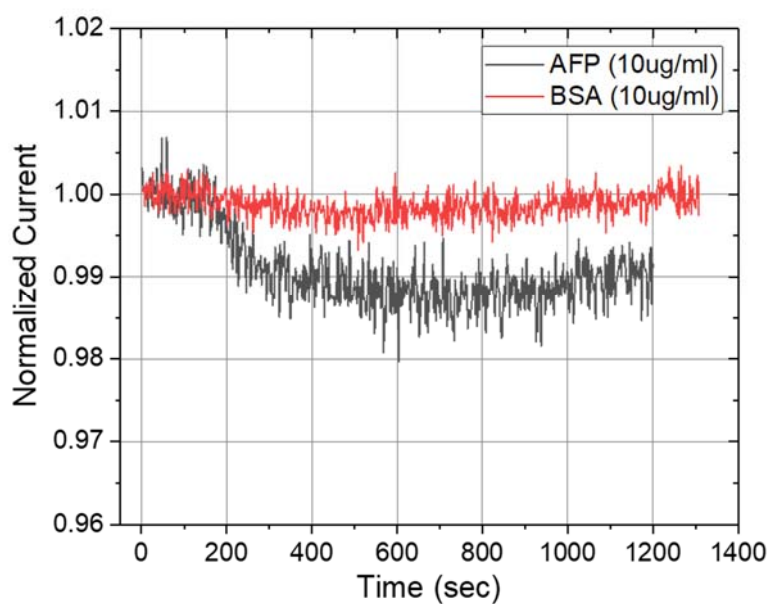


Figure 4-8 Real time measurement of the changes of current under deactivation of NHS ester by BSA; 1) The current change by nonspecific protein, such as BSA, decreases after deactivation. 2) It also diminishes the current change by AFP which is the target molecule.

4.5 Conclusion of chapter 4

To enhance the performance of the developed device, four strategies using the electrical and the chemical method have been attempted. Those methods were expected to improve the sensitivity of sensor device utilizing the antigen-antibody reaction. Although it was expected that the increased change of the current during the antibody-antigen reaction could be obtained by introducing the electrical and the chemical methods, actual improvements in the current response were minimal. The reasons may be qualitatively summarized as follows;

At first, it has been reported that the transient measurement on the developed devices can enhance the sensor performance when the DNA and the aptamer was chosen the probe molecules [7][8] as shown in Fig 4-9. However, in the experiment when the antibody was chosen as the probe molecule, the transient measurement could not improve the performance of the sensor device. This is can be understood that the size of the antibody is much larger than that of the DNA and the aptamer. Once the electric step pulse was applied, the counter ions were repelled from the channel and the electrode surface during the transient period. The region (extended Debye length) without the counter ions is not sufficiently long enough to de-screen the charges of the antigen bound to the antibody. Because the size of the antibody is comparable or longer than

Dedye length so the location of the target molecules is relatively further away from the channel compared with the case of, the DNA and the aptamer.

Secondly, the ACEF method based on the AC signal with the high amplitude of the voltage and the high frequency forms the flow in the buffer electrolyte solution. Once the solution temperature nearby the electrode increases by the Joule heating, it generates the flow in the solution. This stirring-like flow increases the concentration of the molecules at the channel surface, thereby the binding ratio of the reaction between the target and the probe molecule can be enhanced effectively. However, under the ACEF bias condition, as the temperature of the solution nearby the channel and the electrode surface increases, the antibody proteins might be denaturalized. As a result, the affinity of the antibody may be degraded.

Even though two strategies, the transient measurement and the ACEF method are appropriate for the small target molecules, not susceptible to the temperature change of the solution, those methods may not applicable for the antibody-antigen reaction where the antibody size is large and affinity is degraded by the solution temperature.

Thirdly, after substituting the MPA linker with the MUA linker (the longer one), the amount of the current change diminished. It is because the longer chain length of the MUA have the antibody far away from the channel surface

while the binding kinetics is improved.

The last method is to reduce the nonspecific binding by deactivating the NHS ester sites with the non-reactive proteins (BSA in our work). After deactivating the NHS ester sites, the amount of the antigen available to bound to the antibody can be increased. However, as shown in the experiment result of the target AFP and the control BSA, the overall change of the current response become smaller. Other strategy for the deactivation of the NHS ester sites are required.

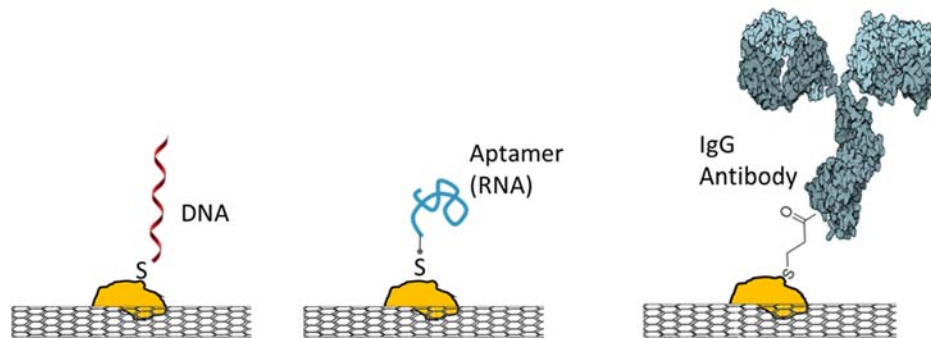


Figure 4-9 Schematic illustration of the DNA, aptamer and antibody immobilized on the AuNP decorated CNT device; 1) DNA or aptamer has an advantage to detect since its size is smaller than that of antibodies. 2) The binding region of probe is near the CNT surface that can be more affected by target molecule. 3) DNA and aptamer do not have degradation in high temperature which is induced by joule heating in ACEF.

Chapter 5

Conclusion

5.1 Summary

Four sub works have been performed to achieve the general sensor platform, called C-chip, based on the antibody antigen reactions.

First, the detail fabrication of the electrical sensor suitable for the sensor array has been set up. The sensor devices have the channel consisting of the AuNP decorated CNN device. The channel was fabricated by utilizing the dip coating method and the thermal evaporation of the gold nanoparticle. The device, which consists of the concentric electrode structure, can operate without a reference electrode which is usually adopted in the conventional electrochemical devices.

Second, the biosensor platform detecting the antibody-antigen proteins has been developed. For the probe molecule, the IgG-type antibody was chosen. To immobilize the antibody on the device channel surface, series of the the proper chemical treatments have been developed.

During the chemical treatments, the chemical effects on the electrical characteristics of the device were analyzed by observing the change of the current response. From the electrical monitoring, it has been shown that our surface treatments of the channel for the bio sensor platform give reliable, stable and uniform channel surface without damage during the treatments.

Third, after immobilizing the antibody on the channel surface of the device, the detecting of the AFP, the antigen of the hepatocellular carcinoma (liver cancer), was performed as an example. The channel current change due to the antigen-antibody reaction has been observed. However, compared with the control experiments done with the BSA as the nonspecific molecules, the sensitivity to the target molecules were regarded to be not enough for practical applications.

Fourth, four strategies, including the electrical and chemical methods to enhance the sensitivity of the sensor device is applied and introduced. Even though the strategies have not given the satisfactory results, many implications from the measurements have been obtained; they are the need of the shortening the antibody, optimization of the chemical treatments of the CNN channel, etc.

5.2 Future work

There may be several rooms for improvements of our sensor platform for antibody antigen reaction. Compared with the DNA and aptamer as the probe molecules, the size of the antibody is generally large. Through this work, it has been uncovered that the detection of the antigen by utilizing the charge of the antigen bound to the antibody is difficult in our sensor platform. Therefore, if a smaller antibody than the IgG-type antibody is used, the higher sensitivity and better device performance can be achieved.

Additionally, the immobilization process of the antibody on the AuNP surface should be improved. The process step requires a long process time with big attention. If the probe molecule has the thiol group at the end of the structure, the direct immobilization process can be possible excluding the complex chemical treatments. Without any linker formation, the probe molecule can be immobilized on the channel surface directly and straightly.

The probe molecule satisfying the abovementioned conditions has been assembled by Professor Chung's laboratory (Medical school of Seoul national university) [38]. The Thiol-terminated scFv-antibody facilitating the epitope of the antibody has been synthesized to have the thiol group at the end of the structure. The scFv-antibody is the small probe molecule, to make it even better, which can be immobilized on the AuNP channel surface directly. It is

expected that the sensitivity of the sensor device can be enhanced after introducing the scFv-antibody on to the device platform.

References

- [1] H. Katz, “Chemically Sensitive Field-Effect Transistors and Chemiresistors: New Materials and Device Structures,” *Electroanalysis*, vol. 16, no. 22, pp. 1837–1842, Nov. 2004.
- [2] X.-J. Huang and Y.-K. Choi, “Chemical sensors based on nanostructured materials,” *Sensors Actuators B Chem.*, vol. 122, no. 2, pp. 659–671, Mar. 2007.
- [3] D. W. Kim *et al.*, “Self-gating effects in carbon nanotube network based liquid gate field effect transistors,” *Appl. Phys. Lett.*, vol. 93, no. 24, p. 243115, 2008.
- [4] S. M. Seo *et al.*, “Carbon Nanotube-Based CMOS Gas Sensor IC: Monolithic Integration of Pd Decorated Carbon Nanotube Network on a CMOS Chip and Its Hydrogen Sensing,” *IEEE Trans. Electron Devices*, vol. 58, no. 10, pp. 3604–3608, Oct. 2011.
- [5] J. H. Cheon *et al.*, “Electrical Characteristics of the Concentric-Shape Carbon Nanotube Network Device in pH Buffer Solution,” *IEEE Trans. Electron Devices*, vol. 57, no. 10, pp. 2684–2689, Oct. 2010.
- [6] J. W. Ko *et al.*, “Multi-order dynamic range DNA sensor using a gold

- decorated SWCNT random network.,” *ACS Nano*, vol. 5, no. 6, pp. 4365–72, Jun. 2011.
- [7] J.-M. Woo, S. H. Kim, H. Chun, S. J. Kim, J. Ahn, and Y. J. Park, “Modulation of molecular hybridization and charge screening in a carbon nanotube network channel using the electrical pulse method.,” *Lab Chip*, vol. 13, no. 18, pp. 3755–63, Sep. 2013.
- [8] W. C. Lee, H. Lee, J. Lim, and Y. J. Park, “An effective electrical sensing scheme using AC electrothermal flow on a biosensor platform based on a carbon nanotube network,” *Appl. Phys. Lett.*, vol. 109, no. 22, p. 223701, Nov. 2016.
- [9] J.-H. Kwon, K.-S. Lee, Y.-H. Lee, and B.-K. Ju, “Single-Wall Carbon Nanotube-Based pH Sensor Fabricated by the Spray Method,” *Electrochem. Solid-State Lett.*, vol. 9, no. 9, p. H85, 2006.
- [10] N. Izard *et al.*, “Semiconductor-enriched single wall carbon nanotube networks applied to field effect transistors,” *Appl. Phys. Lett.*, vol. 92, no. 24, p. 243112, 2008.
- [11] E. Y. Jang, T. J. Kang, H. W. Im, D. W. Kim, and Y. H. Kim, “Single-walled carbon-nanotube networks on large-area glass substrate by the dip-coating method,” *Small*, vol. 4, no. 12, pp. 2255–2261, 2008.
- [12] S. M. Seo *et al.*, “Statistical property of the effect of Au nanoparticle

- decoration on the carbon nanotube network,” *Appl. Phys. Lett.*, vol. 98, no. 14, p. 143106, 2011.
- [13] A. Star, V. Joshi, S. Skarupo, D. Thomas, and J.-C. P. Gabriel, “Gas sensor array based on metal-decorated carbon nanotubes,” *J. Phys. Chem. B*, vol. 110, no. 42, pp. 21014–21020, 2006.
- [14] M. Muratsugu *et al.*, “Quartz crystal microbalance for the detection of microgram quantities of human serum albumin: relationship between the frequency change and the mass of protein adsorbed,” *Anal. Chem.*, vol. 65, no. 20, pp. 2933–7, Oct. 1993.
- [15] D. R. Kauffman and A. Star, “Chemically induced potential barriers at the carbon nanotube-metal nanoparticle interface,” *Nano Lett.*, vol. 7, no. 7, pp. 1863–1868, 2007.
- [16] Y. Sato *et al.*, “Early Recognition of Hepatocellular Carcinoma Based on Altered Profiles of Alpha-Fetoprotein,” *N. Engl. J. Med.*, vol. 328, no. 25, pp. 1802–1806, Jun. 1993.
- [17] R. J. Chen *et al.*, “Noncovalent functionalization of carbon nanotubes for highly specific electronic biosensors,” *Proc. Natl. Acad. Sci. U. S. A.*, vol. 100, no. 9, pp. 4984–4989, 2003.
- [18] S. Choi and J. Chae, “Methods of reducing non-specific adsorption in microfluidic biosensors,” *J. Micromechanics Microengineering*, vol.

20, no. 7, p. 75015, Jul. 2010.

- [19] N. Gao, W. Zhou, X. Jiang, G. Hong, T. M. Fu, and C. M. Lieber, “General strategy for biodetection in high ionic strength solutions using transistor-based nanoelectronic sensors,” *Nano Lett.*, vol. 15, no. 3, pp. 2143–2148, 2015.
- [20] Z. Liu, S. Tabakman, K. Welsher, and H. Dai, “Carbon nanotubes in biology and medicine: In vitro and in vivo detection, imaging and drug delivery,” *Nano Res.*, vol. 2, no. 2, pp. 85–120, 2009.
- [21] L. N. Cella, W. Chen, N. V Myung, and A. Mulchandani, “Single-walled carbon nanotube-based chemiresistive affinity biosensors for small molecules: ultrasensitive glucose detection.,” *J. Am. Chem. Soc.*, vol. 132, no. 14, pp. 5024–6, Apr. 2010.
- [22] M. S. Szymanski and R. a Porter, “Preparation and quality control of silver nanoparticle-antibody conjugate for use in electrochemical immunoassays.,” *J. Immunol. Methods*, vol. 387, no. 1–2, pp. 262–9, Jan. 2013.
- [23] S. Chen, L. Liu, J. Zhou, and S. Jiang, “Controlling antibody orientation on charged self-assembled monolayers,” *Langmuir*, vol. 19, no. 7, pp. 2859–2864, 2003.
- [24] P. Bhadra, M. S. Shajahan, E. Bhattacharya, and A. Chadha, “Studies

- on varying n-alkanethiol chain lengths on a gold coated surface and their effect on antibody–antigen binding efficiency,” *RSC Adv.*, vol. 5, no. 98, pp. 80480–80487, 2015.
- [25] S. N. Kim, J. F. Rusling, and F. Papadimitrakopoulos, “Carbon Nanotubes for Electronic and Electrochemical Detection of Biomolecules.,” *Adv. Mater.*, vol. 19, no. 20, pp. 3214–3228, Oct. 2007.
- [26] S. Choi and J. Chae, “A regenerative biosensing surface in microfluidics using electrochemical desorption of short-chain self-assembled monolayer,” *Microfluid. Nanofluidics*, vol. 7, no. 6, pp. 819–827, 2009.
- [27] X. Duan, Y. Li, N. K. Rajan, D. a. Routenberg, Y. Modis, and M. a. Reed, “Quantification of the affinities and kinetics of protein interactions using silicon nanowire biosensors,” *Nat. Nanotechnol.*, vol. 7, no. 6, pp. 401–407, May 2012.
- [28] S. Loire, P. Kauffmann, I. Mezić, and C. D. Meinhart, “A theoretical and experimental study of ac electrothermal flows,” *J. Phys. D. Appl. Phys.*, vol. 45, no. 18, p. 185301, 2012.
- [29] M. Sigurdson, D. Wang, and C. D. Meinhart, “Electrothermal stirring for heterogeneous immunoassays.,” *Lab Chip*, vol. 5, no. 12, pp.

1366–1373, 2005.

- [30] M. L. Y. Sin, V. Gau, J. C. Liao, and P. K. Wong, “Electrothermal fluid manipulation of high-conductivity samples for laboratory automation applications,” *JALA - J. Assoc. Lab. Autom.*, vol. 15, no. 6, pp. 426–432, 2010.
- [31] Y. Lu *et al.*, “AC Electrokinetics of Physiological Fluids for Biomedical Applications.,” *J. Lab. Autom.*, 2014.
- [32] D. a C. Beck and V. Daggett, “Methods for molecular dynamics simulations of protein folding/unfolding in solution.,” *Methods*, vol. 34, no. 1, pp. 112–20, Sep. 2004.
- [33] A. J. Di Pasqua, R. E. M. Ii, Y. Ship, J. C. Dabrowiak, and T. Asefa, “Preparation of antibody-conjugated gold nanoparticles,” *Mater. Lett.*, vol. 63, no. 21, pp. 1876–1879, 2009.
- [34] G. J. Wegner, H. J. Lee, and R. M. Corn, “Characterization and optimization of peptide arrays for the study of epitope-antibody interactions using surface plasmon resonance imaging.,” *Anal. Chem.*, vol. 74, no. 20, pp. 5161–8, Oct. 2002.
- [35] R. a Sperling and W. J. Parak, “Surface modification, functionalization and bioconjugation of colloidal inorganic nanoparticles.,” *Philos. Trans. A. Math. Phys. Eng. Sci.*, vol. 368, no. 1915, pp. 1333–1383,

2010.

- [36] X. Wang *et al.*, “Carbon nanotube-DNA nanoarchitectures and electronic functionality.,” *Small*, vol. 2, no. 11, pp. 1356–65, Nov. 2006.
- [37] S. Hrapovic, E. Majid, Y. Liu, K. Male, and J. H. T. Luong, “Metallic nanoparticle-carbon nanotube composites for electrochemical determination of explosive nitroaromatic compounds,” *Anal. Chem.*, vol. 78, no. 15, pp. 5504–5512, 2006.
- [38] A. Yoon, J. W. Shin, S. Kim, H. Kim, and J. Chung, “Chicken scFvs with an artificial cysteine for site-directed conjugation,” *PLoS One*, vol. 11, no. 1, p. e0146907, Jan. 2016.

초록

바이오센서는 특정 DNA 서열 또는 단백질 같은 바이오 분자를 검출하거나 정량화 할 수 있게 설계된 소자이다. 본 논문에서는 탄소나노튜브를 기반으로 한 전기적 단백질 센서 플랫폼의 개발 방법을 제안한다. 이를 위해서 수행한 연구는 크게 세 가지로 나뉜다.

첫 번째, 반도체 표준 공정을 통하여 동심원 전극으로 구성된 소자를 만들고 딥 코팅 방식을 사용하여 전극 사이에 탄소나노튜브 채널을 형성한다. 그리고 탄소나노튜브 채널 위에 금 나노입자를 증착하여 소자의 안정성과 균일성을 확보하였다.

두 번째, 금 나노입자가 증착된 탄소나노튜브 소자를 단백질 센서로 활용하기 위해서 소자에 표면 처리를 하여 금 나노입자 위에 항체를 고정화하였다. 사용한 항체는 간암 바이오마커인 alpha fetoprotein (AFP) 단백질과 결합할 수 있는 탐지 생체분자이다.

세 번째, 항원 항체 반응으로 인해 발생하는 탄소나노튜브의 전류 변화를 증가시키기 위해 전기적 방법과 화학적 방법을 적용해 보았다.

본 연구를 통하여 우리는 탄소나노튜브를 기반으로 한 단백질 센서 플랫폼을 개발하였고, 이를 이용하여 다양한 단백질 물질들에 대해 충분한 감도와 신뢰성을 갖는 바이오센서를 제작하여 실시간 전기적 검출을 진행하는데 기여할 수 있을 것으로 기대한다.

주요어 : 탄소나노튜브, 금 나노입자, 단백질 센서, 항원 고정화, 간암 바이오마커.

학번 : 2008-20957